

# Superconductor-Insulator Transition in Weakly Monitored Josephson Junction Arrays

Purnendu Das<sup>1</sup>, Sumilan Banerjee<sup>2</sup>

<sup>1</sup>*Department of Physics, Indian Institute of Science, Bangalore 560012, India,*

<sup>2</sup>*Centre for Condensed Matter Theory, Department of Physics, Indian Institute of Science, Bangalore 560012, India\**

(Dated: December 9, 2024)

Control and manipulation of quantum states by measurements and bath engineering in open quantum systems, and associated phenomena, such as measurement-induced phase transitions, have emerged as new paradigms in many-body physics. Here, taking a prototypical example of Josephson junction arrays (JJAs), we show how repetitive monitoring can transform an insulating state in these systems to a superconductor and vice versa. To this end, we study the effects of continuous weak measurements and feedback control on isolated JJAs in the absence of any external thermal bath. The monitoring due to combined effect of measurements and feedback, inducing non-unitary evolution and dissipation, leads to a long-time steady state characterized by an effective temperature in a suitably defined semiclassical limit. However, we show that the quantum dissipation due to monitoring has fundamental differences with equilibrium quantum and/or thermal dissipation in the well-studied case of JJAs in contact with an Ohmic bath. In particular, using a variational approximation, and by considering the semiclassical, strong measurement/feedback and weak-coupling limits, we demonstrate that this difference can give rise to re-entrant steady-state phase transitions, resulting in transition from an effective low-temperature insulating normal state to superconducting state at intermediate temperature. Our work emphasizes the role of quantum feedback, that acts as an additional knob to control the effective temperature of non-equilibrium steady state leading to a phase diagram, not explored in earlier works on monitored and open quantum systems.

Measurement plays an important role at the foundation of quantum mechanics<sup>1-3</sup>. Measurement abruptly collapses a wave function making the evolution of quantum state non-unitary, and can have strong interplay with quantum entanglement. For instance, local measurements can disentangle an entangled state. In recent years, the competition between entangling unitary evolution and disentangling local measurements has been shown to lead to unusual dynamical phase transitions, the so-called ‘measurement-induced phase transition’ (MIPT) in quantum many-body systems subjected to repeated measurements<sup>4-16</sup>. MIPT is an entanglement phase transition as a function of measurement strength between a volume-law to area-law entangled long-time steady states<sup>4-16</sup>. MIPT is realized at the level of a typical individual quantum trajectory that is characterized by keeping the full record of all the measurement outcomes. Here we ask whether repeated measurements can induce steady-states and associated phase transitions that are more conventional, like zero-temperature equilibrium quantum phase transition (QPT) between symmetry-broken and unbroken states, even at the level of trajectory average quantities. For instance, can a system be transformed from its normal state to superconducting state and vice versa, by performing repeated measurements?

To address these questions, we consider the paradigmatic system of Josephson junction arrays (JJAs)<sup>17-20</sup>, that realizes a superconductor-normal state, namely a superconductor-insulator (SI) quantum phase transition. JJAs, physical realizations of the Quantum XY model<sup>20-22</sup>, are artificially created as the networks of mesoscopic superconducting (SC) islands, interconnected by Josephson junctions, or may be realized as effective models for granular superconductors<sup>23-27</sup>. JJAs undergo

SI transition as a function of the ratio of the charging energy ( $E_c$ ), that controls the quantum fluctuations of Cooper pair number in an island, and the Josephson coupling strength ( $J$ ). Remarkably, dissipation, either originating intrinsically<sup>20,23,28</sup> or introduced in a controlled manner<sup>29-31</sup> in experiments, is known to play important role in determining the nature of the thermodynamic SI transition. The effects of dissipation on JJAs, modeled by JJAs coupled to various types of thermal and quantum baths<sup>20</sup>, e.g., Ohmic baths, have been widely studied<sup>32-36</sup>. In this work, we study the effects of continuous weak measurement and feedback on otherwise isolated JJAs in the absence of any external thermal bath. The measurements and feedback at a very basic level act as a source of non-unitary evolution and dissipation, and lead to an effective temperature description in a suitably defined classical or ‘high-temperature limit’. However, we show that ‘quantum dissipation’ due to monitoring, in general, has essential differences with well-studied cases of equilibrium quantum and/or thermal dissipation in JJAs. In particular, we demonstrate that this difference can give rise to a steady-state phase transition from an effective low-temperature insulating normal state to superconducting state at higher temperatures.

Bath engineering to manipulate dissipation and phenomena beyond equilibrium has been discussed in the context of Lindblad description of open systems in many earlier works<sup>37-47</sup>, e.g., in the pioneering works by Diehl et al.<sup>38,40</sup> on interacting bosons with dissipative coupling to the particle current. This model is closely connected to our monitored JJAs model. In the dissipative Bose-Hubbard model, a pure Bose-Einstein condensate (BEC) in the non-interacting limit, and a weakly mixed superfluid state in the presence of interaction are induced by the engineered dissipation. In the interacting superfluid

state, an effective temperature emerges due to the constraint on the number of particles or the chemical potential, that is controlled by the interaction strength. In contrast, in our model we envisage a situation where the number of cooper pairs on each mesoscopic JJ is effectively unbounded. We show that quantum feedback in this situation acts as an extra handle to control the effective temperature of non-equilibrium steady state leading to a phase diagram with re-entrant as well as high-to-low-temperature superconductor-to-insulator transitions, not realized in earlier works<sup>38,40,42</sup>.

As depicted in Fig.1(a), by generalizing a well-known model of continuous weak position measurement on a single particle<sup>48</sup>, we construct a model of monitored JJA, where the phase difference between any two neighboring SC island across a JJ link is weakly measured repeatedly with strength  $\Delta^{-1}$  through coupling with a detector or meter, and, subsequently, a feedback<sup>3,48</sup> with strength  $\gamma$  is applied. The measurement of phase difference plays a similar role to the dissipative current coupling in Refs.38,40,42. In the presence of JJ coupling, the measurement is naively expected to enforce a fixed phase difference by weakly collapsing the wave function, and thus favor a globally phase-coherent SC steady-state by suppressing quantum fluctuation of the SC phase when repeated many times across the JJA. The feedback acts as a source of dissipation and gives rise to an effective temperature  $T_{eff} \sim \Delta^{-1}/\gamma$ , similar to a quantum heating phenomenon<sup>49,50</sup>.  $T_{eff}$  is defined via an emergent fluctuation-dissipation ratio (FDR) for the long-time steady state for low-energy excitations and a high-temperature or classical limit. In the latter regime FDR is identical to that of the high-temperature limit of the JJAs with standard Ohmic dissipation<sup>33,34</sup>. However, in the effective low-temperature or quantum limit, we find that the FDR, and thus the quantum dissipation, for the steady state of the monitored JJA is fundamentally different from the Ohmic JJA.

Within a variational self-consistent harmonic approximation (SCHA), this difference in the nature of dissipation leads to a phase diagram of monitored JJA, as a function of effective dissipation strength  $\gamma$  or effective temperature, very distinct from that of dissipative JJA, as shown in Figs.1(b-e). In particular, below a threshold value of JJ coupling  $(J/E_c)_{th}$ , the system remains insulating irrespective of  $\gamma$ . This is unlike Ohmic JJA where dissipation, above a threshold value restores superconductivity at low temperature [Fig.1(c)] by inhibiting quantum phase fluctuations. Moreover, re-entrant insulator-SC-insulator transitions are realized for monitored JJA above  $(J/E_c)_{th}$  [Fig.1(b)]. Similarly, qualitatively different phase diagrams for monitored and Ohmic JJAs [Figs.1(d,e)] are obtained as a function of effective temperature for a fixed dissipation. Again, above a threshold  $(J/E_c)_{th}$ , re-entrant transitions appear leading to a low-temperature insulator to high-temperature SC transition. We verify our conclusions by going beyond SCHA, in the (i) high-temperature or classical, (ii)

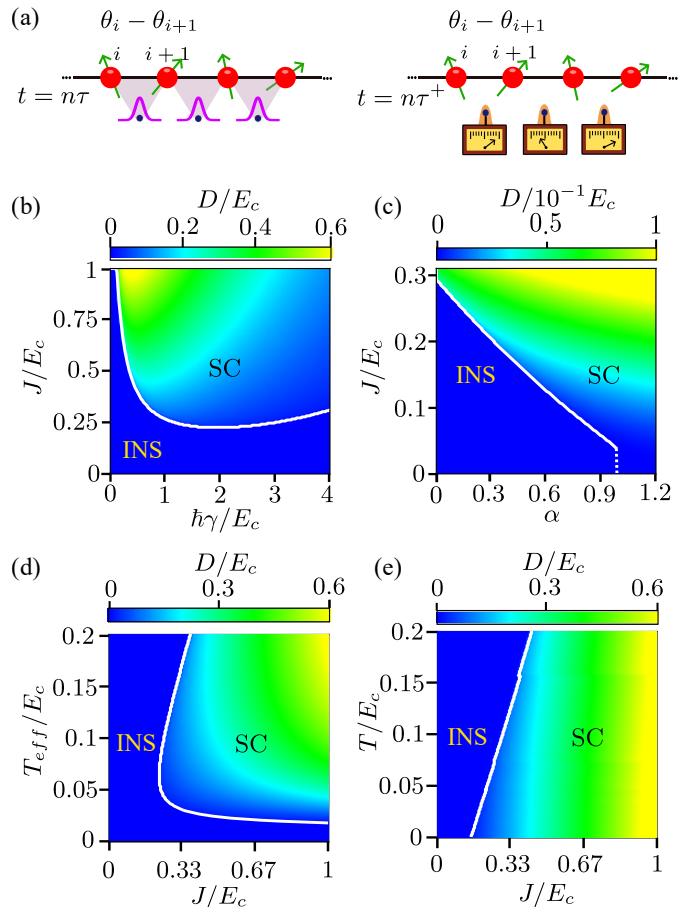


**FIG. 1. Monitored Josephson junction array (JJA) and phase diagrams:** (a) The schematics of the continuous weak measurement setup for a one-dimensional (1d) JJA is shown. For the  $n$ -th measurement the detectors on the JJ links, e.g.,  $(i, i + 1)$ , prepared in a Gaussian state just before ( $t = n\tau^-$ ) the measurement, are coupled to the JJ phase differences  $(\theta_i - \theta_{i+1})$  at time  $t = n\tau$ . The detectors are subsequently decoupled and measured at time  $t = n\tau^+$ . Further, a feedback is applied using the measurement outcomes (see the main text). (b) The phase diagram within the self-consistent harmonic approximation (SCHA) as a function of JJ coupling  $J$  and feedback  $\gamma$  exhibits superconductor (SC)-insulator (INS) transition, as indicated by the superfluid stiffness  $D$  (color) for a fixed measurement strength  $\hbar\Delta^{-1}/E_c = 0.5$ . (c) The  $J - \gamma$  phase diagram of the monitored JJA is contrasted with zero-temperature phase diagram in the  $J$ -dissipation ( $\alpha$ ) plane for Ohmic JJA (see Supplementary Sec.S3). (d) Phase diagram for monitored JJA as a function of effective temperature  $T_{eff}$  and  $J$  is compared with the  $T$  vs.  $J$  phase diagram of Ohmic JJA for  $\alpha = 0.5$  in (e).

strong feedback and measurement, and (iii) weak JJ coupling limits. We show that the behavior in large feedback/measurement limit, and the renormalization group (RG) flow for the weak-coupling limit of the monitored JJA are fundamentally different from those in Ohmic JJA, in conformity with the SCHA. On the contrary,

a stochastic Langevin description, with classical a FDR controlled by  $\gamma$  and  $T_{eff}$ , emerges in the monitored system in the classical limit at high temperature, leading to SI transition identical to finite-temperature SI transition in Ohmic JJAs.

### Model of monitored JJA

We consider a system-detector model Fig.1(a) with Hamiltonian  $\mathcal{H}(t) = \mathcal{H}_s + \mathcal{H}_{sd}(t)$ , where the system of JJA<sup>20</sup> is described by  $\mathcal{H}_s = (1/2) \sum_i E_c \hat{n}_i^2 + J \sum_{\langle ij \rangle} (1 - \cos(\hat{\theta}_i - \hat{\theta}_j))$ , with on-site charging energy  $E_c$  and nearest-neighbor JJ coupling  $J$  on a hypercubic lattice in  $d$  dimension with spacing  $a$  and  $L^d$  sites. The Cooper pair number  $\hat{n}_i$  and the phase  $\hat{\theta}_i$  operator on each SC island  $i$  satisfies  $[\hat{\theta}_i, \hat{n}_j] = i\delta_{ij}$ . The JJA is coupled via  $\mathcal{H}_{sd}(t) = \sum_{\langle ij \rangle} \delta(t - n\tau) \Delta \hat{\theta}_{ij} \hat{p}_{ij,n}$  to a set of detectors or ‘meters’ at regular intervals  $t = n\tau$  through the phase difference  $\Delta \hat{\theta}_{ij} = \hat{\theta}_i - \hat{\theta}_j$  across JJ at the link  $\langle ij \rangle$ . The meters are quantum particles with (dimensionless) position  $\hat{x}_{ij,n}$  and momenta  $\hat{p}_{ij,n}$  satisfying  $[\hat{x}_{ij}, \hat{p}_{kl}] = i\delta_{\langle ij \rangle, \langle kl \rangle}$ . The meters are prepared in a Gaussian state  $\psi_{ij}(x_{ij,n}) = (\pi\sigma)^{-1/4} \exp(-x_{ij,n}^2/2\sigma)$  before the measurement at  $t = n\tau^-$ . The weak measurements on the system comprise projective measurements of the position of the meters at  $t = n\tau^+$  leading to stochastic outcomes  $\xi_{ij,n}$  at the  $n$ -th set of measurements on all the links. The full record of all the measurement outcomes  $\{\xi_{ij,n}\}$  over a time constitutes a quantum trajectory. However, these repeated measurements with unbounded Cooper pair number, and thus unbounded charging energy in the JJA model, lead to indefinite heating up of the system, as known for the case of weak position measurements of a single particle<sup>48</sup>. Hence, we apply a unitary feedback<sup>3,48</sup>  $U_{ij,n} = e^{i\gamma\tau\xi_{ij,n}(\hat{n}_i - \hat{n}_j)}$  after each measurement with strength  $\gamma$ .

As we show in the Appendix A, in the above measurement model, one can obtain a non-unitary time evolution of the (unnormalized) density matrix  $\rho(t)$  of the system. Moreover, in the limit of continuous weak measurement limit<sup>48</sup>,  $\tau \rightarrow 0$ ,  $\sigma \rightarrow 0$  such that  $\sigma\tau = \Delta$  is finite, the dynamics of the JJA system for a particular quantum trajectory  $\xi_{ij}(t)$  over a time interval  $t_f$  can be described by a Schwinger-Keldysh (SK) [Fig.2(a)] generating function  $Z[\xi] = \text{Tr}[\rho(t_f, \{\xi\})] = \int \mathcal{D}\theta e^{iS[\theta, \xi]/\hbar} \langle \theta_+(t_0) | \rho_0 | \theta_-(t_0) \rangle$ , which is essentially the Born probability of the trajectory. Here  $\Delta^{-1}$  is the measurement strength and  $\rho_0$  is the density matrix of the system at the initial time  $t_0$ . We assume that the non-equilibrium steady state for  $t_f \rightarrow \infty$  does not depend on  $\rho_0$ . The SK action is given by

$$S[\theta, \xi] = \int_{t_0}^{t_f} dt \left[ \sum_{i,s} s \left\{ \frac{\hbar^2 \dot{\theta}_{is}^2}{2E_c} + \frac{\hbar^2 \gamma}{E_c} \dot{\theta}_{is} \sum_{j \in \text{nn}_i} \xi_{ij}(t) \right\} - \sum_{\langle ij \rangle, s} s \left\{ J (1 - \cos \Delta \theta_{ij,s}) - \frac{is\hbar}{2\Delta} (\xi_{ij}(t) - \Delta \theta_{ij,s})^2 \right\} \right]. \quad (1)$$

Here  $s = \pm(\pm 1)$  denotes the forward and backward

branches of SK contour [Fig.2(a)], and  $\dot{\theta}_{is} = d\theta_{is}/dt$  and  $\text{nn}_i$  refers to sites nearest neighbor to  $i$ .

### Self-consistent harmonic approximation (SCHA)

We first use a self-consistent harmonic approximation (SCHA) where a variational action  $S_v$  is obtained by replacing JJ coupling term  $J(1 - \cos \Delta \theta_{ij,s})$  in Eq.(1) with a harmonic term  $D_{ij,s}(t) \Delta \theta_{ij,s}^2 / 2$  having the variational parameter  $D_{ij,s}(t)$  (see Appendix B). The variational Born probability  $Z_v[\xi] = \exp(-F_v[\xi])$  is maximized by minimizing  $F_v = -(i/\hbar) \langle (S - S_v) \rangle_v - \ln Z_v$  with respect to  $D_{ij,s}(t)$ . As discussed in the Appendix B, we further assume a spatio-temporal translationally invariant steady state, and solve the self-consistency condition after averaging over all the trajectories, i.e.,

$$D = J \exp(-\overline{\langle \Delta \theta_{ij,s}^2(t) \rangle_v} / 2), \quad (2)$$

where  $\overline{\langle \dots \rangle_v}$  denotes trajectory averaged expectation value. The self-consistent parameter  $D$  gives the superfluid stiffness and demarcates between superconductor ( $D \neq 0$ ) and normal state ( $D = 0$ ), e.g., the insulator.

### Steady-state FDR and effective temperature

As discussed in the Appendix B, the effective self-consistent harmonic action for the trajectory-averaged steady state can be written as

$$\frac{1}{\hbar} S_{eff} = \frac{1}{2} \sum_q \theta^T(-q) G^{-1}(q) \theta(q) \quad (3)$$

in terms of Fourier transform  $\theta^T(q) = (\theta_c(q), \theta_q(q))$  of the classical and quantum components  $\theta_c$  and  $\theta_q$ , after Keldysh rotation<sup>50</sup>  $\theta_{is}(t) = \theta_{ic}(t) + s\theta_{iq}(t)$ ;  $q = (\mathbf{q}, \omega)$  denotes momentum and frequency, and  $\sum_q \equiv \sum_{\mathbf{q}} \int_{-\infty}^{\infty} (d\omega/2\pi)$ . The effective inverse propagator  $G^{-1}(q)$  has the usual causal Keldysh structure<sup>50</sup>, namely  $[G^{-1}]_{cc}(q) = 0$ , the retarded (advanced) components  $[G^{-1}]_{qc(cq)} = [G^{-1}]^{R(A)}(q) = (2/\hbar)[(\hbar\omega^\pm)^2/E_c - (D \mp i\hbar^2\gamma\omega^\pm/E_c)K(\mathbf{q})]$ , and  $[G^{-1}]_{qq}(q) = [G^{-1}]^K(q) = (2i/\hbar)K(\mathbf{q})(\hbar\Delta^{-1} + \hbar^3\gamma^2\omega^2/E_c^2\Delta^{-1})$ . Here  $K(\mathbf{q}) = 2d - 2\sum_{\mu=1}^d \cos(q_\mu a)$  and  $\omega^\pm = \omega \pm i\eta$  with  $\eta \rightarrow 0^+$ . The propagator  $G(q)$  can be used to compute  $\overline{\langle \Delta \theta_{ij,s}^2(t) \rangle_v} = (E_c/4dD)(\Delta^{-1}/\gamma) + (\gamma/2\Delta^{-1})$ , and thus to obtain  $D$  self consistently from Eq.(2) (Appendix B).

Using  $G(q)$ , we can obtain a FDR for the steady state from  $G^K(q)/[G^R(q) - G^A(q)] = 2T_{eff}/\hbar\omega + \hbar\omega/8T_{eff}$ , where

$$T_{eff} = \frac{\Delta^{-1}}{4\gamma} E_c \quad (4)$$

is an effective temperature that becomes unbounded in the absence of the feedback, as mentioned earlier. Moreover, the phase fluctuation can be written solely in terms of the combination  $(\Delta^{-1}/\gamma) \propto T_{eff}$ , i.e.  $\overline{\langle \Delta \theta_{ij,s}^2(t) \rangle_v} = (T_{eff}/dD) + (E_c/8T_{eff})$ . The steady-state FDR can be compared with usual FDR for thermal equilibrium at temperature  $T$ , namely  $\text{coth}(\hbar\omega/2T) = 2T/\hbar\omega + \hbar\omega/6T +$

$\dots$  ( $k_B = 1$ ), which is applicable to Ohmic JJA<sup>33,34</sup> (Supplementary Sec.S3). Thus the steady-state FDR coincides with the thermal FDR with  $T = T_{eff}$ , for an effective high-temperature limit  $T_{eff} \gg \hbar\omega$ , or equivalently, for low energy ( $\omega \rightarrow 0$ ) or the semiclassical limit ( $\hbar \rightarrow 0$ ). However, unlike the Ohmic JJA<sup>33,34</sup>, the temperature in the monitored JJA emerges in the absence of any thermal bath, purely from measurement, feedback and quantum fluctuations<sup>51</sup>. Moreover, the steady-state FDR is completely different from the thermal FDR at low effective temperatures, leading to fundamentally different quantum dissipation and qualitatively distinct phase diagram of Fig.1 for monitored JJA, compared to Ohmic JJA. In particular, there is no analogous *zero-temperature* limit for the monitored model compared to the Ohmic JJA, as discussed in Supplementary Sec.S41. In Supplementary Sec.S31, comparing the propagator  $G(q)$  of the monitored and Ohmic JJAs, we establish the exact equivalence between feedback  $\gamma$  and Ohmic dissipation in the high-temperature limit.

### Phase diagram

We obtain the phase diagrams for the monitored JJA by numerically solving the self-consistency equation of Eq.(2). As shown in Figs.1(b-d), and discussed earlier, the phase diagrams of monitored JJA as a function of  $\gamma$  and  $T_{eff}$ , are compared with the phase diagrams of Ohmic JJA as a function of dissipation strength  $\alpha$  and temperature  $T$ , respectively. Furthermore, we also plot the phase diagram as a function of measurement strength  $\Delta^{-1}$  for a fixed  $\gamma$  in Fig.2(b), and demonstrate the re-entrant transitions for a fixed  $J$  in Figs.2(c,d). As discussed in the Supplementary Sec.S4, for the monitored JJA, the phase boundary between SC and insulating phases, as well as the threshold value of JJ coupling  $(J/E_c)_{th}$  can be obtained analytically, and can be shown to be always first order with a discontinuity in  $D$ . However, the first order nature could be due to the well-known artifact<sup>52,53</sup> of the SCHA near a transition. Nevertheless, the basic structure of the phase diagrams in Figs.1,2, namely the existence of the phases, re-entrant transitions and the threshold  $(J/E_c)_{th}$  are expected to be robust features, beyond the SCHA.

### Semi-classical limit of monitored JJA

Similar to the case of monitored oscillators in Ref.51, we can obtain a non-trivial classical or semiclassical limit  $\hbar \rightarrow 0$ , keeping the ratio  $\Delta/\hbar^2$  fixed, as discussed in the Supplementary Sec.S51. This is achieved by rewriting the action in Eq.(1), in terms  $\theta_{ic}$  and  $\theta_{iq}$ , and expanding up to quadratic order in quantum component  $\theta_{iq}$ . In this limit all the quantum trajectories tend to a single trajectory with measurement outcomes  $\xi_{ij}(t) = \Delta\theta_{ij,c}(t)$ , i.e.,  $\xi_{ij}(t)$  is pinned to the classical component of the phase differences on  $\langle ij \rangle$ . The dynamics of the phases  $\theta_{ic}(t) \equiv \theta_i(t)$  follows standard stochastic Langevin equation,

$$\frac{\hbar^2}{E_c} \ddot{\theta}_i = \sum_{j \in \text{nn}_i} \left[ -\frac{\hbar^2 \gamma}{E_c} \Delta \dot{\theta}_{ij} - J \sin \Delta \theta_{ij} + \eta_{ij} \right] \quad (5)$$

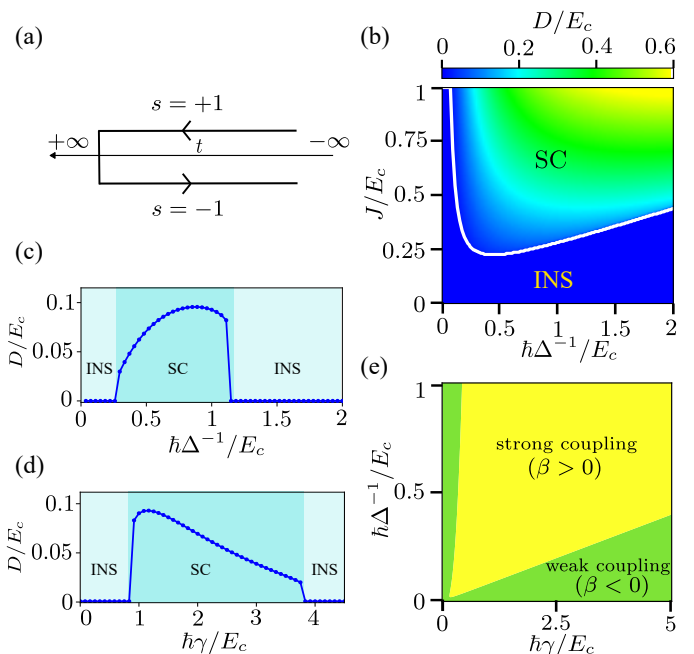


**FIG. 2. Phase diagram of monitored JJA and weak-coupling renormalization group:** (a) Schwinger-Keldysh contour, with forward ( $s = +1$ ) and backward ( $s = -1$ ) branches, used to describe non-unitary dynamics in the long-time steady of monitored JJA. (b) Phase diagram as a function of JJ coupling  $J$  and measurement strength  $\Delta^{-1}$  for a fixed feedback  $\hbar\gamma/E_c = 2$ . The color indicates the superfluid stiffness  $D$  that demarcates between insulating (INS) and superconducting (SC) states. The re-entrant insulator-superconductor-insulator transitions are shown in  $D$  vs.  $\Delta^{-1}$  plot in (c) for  $J/E_c = 0.3$  and  $\hbar\gamma/E_c = 2$ , and in  $D$  vs.  $\gamma$  plot in (d) for  $J/E_c = 0.3$  and  $\hbar\Delta^{-1}/E_c = 0.5$ . (e) The weak-JJ coupling renormalization group qualitatively agrees with the re-entrant nature of the phase diagrams as a function of  $\gamma$  and  $\Delta^{-1}$ . The sign of the  $\beta$  function (color) indicates the flow towards weak coupling ( $\beta < 0$ , insulator) or strong coupling ( $\beta > 0$ , superconductor).

where  $\eta_{ij}$  is a Gaussian white noise originating from fluctuations of  $\theta_{iq}$  with  $\langle \eta_{ij}(t) \eta_{kl}(t') \rangle = (\hbar^2/2\Delta) \delta_{\langle ij \rangle, \langle kl \rangle} \delta(t - t')$ . The latter, along with the damping term in Eq.(5), constitute the classical FDR,  $2(\hbar^2/E_c)\gamma T_{eff} = \hbar^2/2\Delta$ , resulting in the same effective temperature as in Eq.(4). For a meaningful classical limit with non-trivial dynamics, one needs to take  $E_c \propto \hbar^2$  with  $\gamma \sim \mathcal{O}(\hbar^0)$ , as evident from Eq.(5). As a result,  $\langle \Delta \theta_{ij,s}^2 \rangle = T_{eff}/dD + \mathcal{O}(\hbar^2)$  in Eq.(2) and  $D = J \exp(-T_{eff}/dD)$ . The latter exactly matches with the SCHA self-consistency equation of Ohmic JJA in the high-temperature classical limit (Supplementary Sec.S51), implying that the monitored and Ohmic JJAs behave identically in this limit. In fact, the Langevin equation [Eq.(5)] can be used to study this effectively thermal SI transition beyond SCHA, and it will lead to a Berezinskii-Kosterlitz-Thouless (BKT) transition<sup>54,55</sup> in  $d = 2$  and a continuous XY transition in  $d = 3$ .

### Strong feedback and measurement limit of monitored JJA

A similar classical stochastic dynamics for the slow phase modes can also be obtained for strong measurement and feedback strengths,  $\hbar\gamma, \hbar\Delta^{-1} \gg J, E_c$  (Supplementary Sec.S5 2). In this case, one can estimate the renormalization of JJ coupling due to the quantum fluctuations. To this end, we divide the phase variables into fast ( $\omega_c = JE_c/\hbar^2\gamma \lesssim \omega \lesssim \omega_m = \gamma$ ) and slow ( $0 < \omega \lesssim \omega_c$ ) modes, namely,  $\theta_{i\alpha}^>(t) = \int_{\omega_c \leq |\omega| \leq \omega_m} (d\omega/2\pi) e^{-i\omega t} \theta_{i\alpha}(\omega)$  and  $\theta_{i\alpha}^<(t) = \int_{-\omega_c}^{\omega_c} (d\omega/2\pi) e^{-i\omega t} \theta_{i\alpha}^<(\omega)$  ( $\alpha = c, q$ ). We rewrite the action in Eq.(1) in terms of the fast and slow modes and treat the JJ coupling term perturbatively for both slow and fast modes by expanding up to  $\mathcal{O}(\theta_{iq}^{>(<)})$  to capture the leading order effect in  $J$ . Finally we obtain an effective action for the slow modes by integrating out the first modes. Furthermore, in the limit of strong measurement  $\hbar\Delta^{-1} \gg E_c$ , we obtain the same Lagnevin equation of Eq.(1) for  $\theta_{ic}^<(t)$  with the JJ coupling  $J$  replaced by renormalized coupling  $J_{eff} = J(1 - \overline{\langle(\Delta\theta_{ij,c}^>)^2\rangle}/2)$ , where  $\overline{\langle(\Delta\theta_{ij,c}^>)^2\rangle}$  is evaluated for the fast modes (see Supplementary Sec.S5 2). Considering further limiting cases, we obtain  $J_{eff} \simeq (1 - \gamma/4\Delta^{-1})$  for  $\gamma \gg \Delta^{-1}$ , and  $J_{eff} \simeq (1 - (\Delta^{-1}/4\pi\gamma)(E_c/Jd))$  for  $\Delta^{-1} \gg \gamma$ . This implies that  $J_{eff}$  becomes negative for large  $\gamma$  or  $\Delta^{-1}$ , indicating the absence of SC phase in these limits, consistent with the phase diagram within SCHA approximation in Figs.1(b),2(b). Given the equivalence between feedback  $\gamma$  in monitored JJA and dissipation  $\alpha$  in Ohmic JJA, the absence of SC phase in monitored JJA in the strong feedback limit is completely opposite to the case of the strong dissipation limit of Ohmic JJA. In the latter, for large  $\alpha$ ,  $J_{eff} \simeq J(1 - (1/2\alpha d) \ln[1 + (\alpha/2\pi)]) \rightarrow J$ , implying a SC phase for  $\alpha \gg 1^{52}$ , unlike the large  $\gamma$  limit of monitored JJA.

### Weak JJ coupling limit of monitored JJA

Instead of inferring the fate of SC phase from effective classical description of the dynamics of the monitored JJA in the semiclassical or strong feedback and measurement limits, we now look into the perturbative RG flow equation for the JJ coupling  $J$  in the weak-coupling limit  $J \ll E_c$ . We again proceed by defining fast,  $\theta_{is}^>(t) = \int_{\omega_c/b \leq |\omega| \leq \omega_c} (d\omega/2\pi) e^{-i\omega t} \theta_{is}(\omega)$ , and slow,  $\theta_{is}^<(t) = \int_{-\omega_c}^{\omega_c} (d\omega/2\pi) e^{-i\omega t} \theta_{is}(\omega)$ , phase modes. Here  $\omega_c$  is the cutoff frequency, determined by the largest of  $E_c$ ,  $\hbar\gamma$ , and  $\hbar\Delta^{-1}$ . As discussed in the Supplementary Sec.S5 3, the cutoff is systematically rescaled by  $b = e^{\delta l}$  to integrate out the fast modes perturbatively up to first order in  $J/E_c$  for the effective action obtained from trajectory averaged generating function  $\mathcal{Z} = \int \mathcal{D}\xi Z[\xi]$ . After rescaling  $(\theta_{is}(\omega)/b, \omega b, t/b, E_c b) \rightarrow (\theta_{is}(\omega), \omega, t, E_c)$ , to restore the original form of the action and the original cutoff, this results in a renormalized JJ coupling  $J(b) = Jb e^{-\langle(\Delta\theta_{ij,s}^>)^2\rangle/2}$ . Performing infinitesimal RG transformation  $b = e^{\delta l} \approx 1 + \delta l$ , we obtain

the RG flow equation,  $d \ln J / d \ln b = \beta(\tilde{\gamma}, \tilde{\Delta}^{-1})$ , where  $\beta(\tilde{\gamma}, \tilde{\Delta}^{-1}) = [1 - (1/4\pi\tilde{\gamma}d)(\tilde{\Delta}^{-1}/\tilde{\gamma}^2 + (\tilde{\gamma}^2/\tilde{\Delta}^{-1}))]$  with  $(\tilde{\gamma}, \tilde{\Delta}^{-1}) = (\hbar\gamma/E_c, \hbar\Delta^{-1}/E_c)$ . As shown in Fig.2(e), for  $\beta(\tilde{\gamma}, \tilde{\Delta}^{-1}) > 0$ , the JJ coupling flows to strong coupling, presumably, suggesting a SC state, whereas  $\beta(\tilde{\gamma}, \tilde{\Delta}^{-1}) < 0$  implies that  $J$  flows to zero, and indicates an insulating state. Fig.2(e) is consistent with the re-entrant transitions in the SCHA phase diagram [Fig.1(b,d), 2(b)]. This can be contrasted with the case of Ohmic JJA<sup>33,34</sup>, where  $d \ln J / d \ln b = \beta(\alpha) = (1 - 1/\alpha d)$  indicating the flow to strong coupling (SC state) for dissipation  $\alpha > 1/d$  and  $J \rightarrow 0$  for  $\alpha < 1/d$ .

### Conclusions

In this work, we have explored the phase diagram of long-time steady state of weakly and continuously measured JJA with feedback control by looking into quantities, e.g., superfluid density, averaged over quantum trajectories. To this end, we develop a variational self-consistent harmonic approximation based on Born probabilities of quantum trajectories within a Schwinger-Keldysh field theory for non-unitary dynamics in the long-time steady state. Our work reveals an intriguing insulator-superconductor-insulator re-entrant phase transition as a function of the measurement strength or feedback. We find that the monitored model behaves exactly like the JJA with Ohmic dissipation under certain conditions, such as high effective temperatures or semiclassical limit. However, at low effective temperatures, the monitored JJA fundamentally differs from the dissipative model. For example, there are no analogous limits for the monitored model when compared to the zero-temperature Ohmic model. Our work highlights crucial role of feedback to unravel unusual dynamical phase transitions in non-equilibrium steady-state, previously unexplored in engineered open quantum systems, and without any analogue in equilibrium systems, such as low-temperature insulator to high-temperature superconductor transition.

In future, our explicit system-detector model with measurement and feedback can be used to theoretically study the measurement-induced entanglement transition at the level of typical individual trajectory for pure state evolution, or even trajectory-averaged mixed-state transitions in terms of mixed-state entanglement measures such as entanglement negativity. Qualitatively similar models with measurements and feedback control can be experimentally realized in the related systems of transmon qubits.

### ACKNOWLEDGEMENTS

We acknowledge fruitful discussions with Vibhor Singh. PD acknowledges support from Kishore Vaigyanik Protsahan Yojana (KVPY) from DST, Govt. of India. SB acknowledges support from CRG, SERB (ANRF), DST, India (File No. CRG/2022/001062) and STARS, MoE, Govt. of India (File. No. MoE-STARS/STARS-

2/2023-0716).

## Appendix A: Dynamics of monitored JJA

Here we discuss the non-unitary time evolution of the JJA under weak measurements and feedback discussed in the main text [see Fig.1(a)]. Before the  $n$ -th measurements at time  $t = t_n^- = n\tau^-$ , the whole system of JJA and the meters on the links  $\langle ij \rangle$  are described by the density matrix  $\rho_{\text{tot}}(\{\xi_{ij}\}, t_n^-) = \otimes_{\langle ij \rangle} |\psi_{ij,n}\rangle \langle \psi_{ij,n}| \otimes U_s(\tau) \rho(\{\xi_{ij}\}, t_n^-) U_s^\dagger(\tau)$ , where the meters are prepared in a Gaussian states,  $\psi_{ij}(x_{ij,n}) = \langle x_{ij,n} | \psi_{ij} \rangle = (\pi\sigma)^{-1/4} \exp(-x_{ij,n}^2/2\sigma)$ , and the JJA is in a state with (un-normalized) density matrix,  $\rho(\{\xi_{ij}\}, t_n^-)$ . The latter depends on all the previous measurement outcomes  $\xi_{ij}$  till  $t_{n-1}$ , starting with some initial density matrix  $\rho_0$  of the JJA.  $U_s(\tau) = e^{-i\mathcal{H}_s\tau/\hbar}$  is the unitary evolution due to JJA Hamiltonian  $\mathcal{H}_s$ . After the system-detector interaction  $\mathcal{H}_{sd}(t)$  at time  $t = n\tau$ , the position of the meters are measured projectively at  $t = n\tau^+$ , leading to

$$\begin{aligned} \rho_{\text{tot}}(t_n^+) &= \mathcal{P}_n \left[ \prod_{\langle ij \rangle} (e^{-i\Delta\theta_{ij} p_{ij,n}}) \otimes_{ij} |\psi_{ij,n}\rangle \langle \psi_{ij,n}| \right. \\ &\quad \left. \otimes U_s(\tau) \rho(t_n^-) U_s^\dagger(\tau) \prod_{\langle ij \rangle} (e^{i\Delta\theta_{ij} p_{ij,n}}) \right] \mathcal{P}_n \quad (\text{A1}) \end{aligned}$$

where  $\mathcal{P}_n = \otimes_{\langle ij \rangle} |\xi_{ij,n}\rangle \langle \xi_{ij,n}|$  is the projection operator corresponding to the measurement outcomes  $\{\xi_{ij,n}\}$  in the  $n$ -th measurements. The density matrix of the JJA,  $\rho(t_n^+) = \text{tr}_M[\rho_{\text{tot}}(t_n^+)] = (\prod_{\langle ij \rangle} M_{ij,n}) U_s(\tau) \rho(t_n^-) U_s(\tau) (\prod_{\langle ij \rangle} M_{ij,n})$ , is obtained by tracing ( $\text{tr}_M$ ) over the meters, where  $M_{ij,n} = \langle \xi_{ij,n} | e^{-i\Delta\theta_{ij} p_{ij,n}} | \psi_{ij,n} \rangle = (\pi\sigma)^{-1/4} e^{-(\xi_{ij,n} - \Delta\theta_{ij})^2/2\sigma}$  leads to non-unitary evolution of the state of the system due to measurements on the meters. As mentioned in the main text, we further apply a unitary displacement operator  $U_{ij,n} = e^{i\gamma\tau\xi_{ij,n}(\hat{n}_i - \hat{n}_j)}$  as a feedback<sup>3,48</sup> to control the heating of the JJA due to repeated measurements.

Accumulating all the steps of the above weak measurement setup, the density matrix of the JJA after  $M$  measurements, over an interval  $t_f = t_M^+$ , is obtained as

$$\rho(\{\xi\}, t_f) = \left[ \prod_{n=1}^M K(\{\xi_{ij,n}\}) U_s(\tau) \right] \rho_0 \left[ \prod_{n=1}^M U_s^\dagger(\tau) K^\dagger(\{\xi_{ij,n}\}) \right] \quad (\text{A2})$$

where  $K(\{\xi_{ij,n}\}) = \prod_{\langle ij \rangle} U_{ij,n} M_{ij,n}$  and  $\rho_0$  is the initial density matrix at  $t_0$ . Finally, following procedure similar to that for monitored oscillators in Ref.51 (see Supplementary Sec.S1), in the continuous weak measurement limit,  $\tau \rightarrow 0$ ,  $\sigma \rightarrow \infty$  with  $\sigma\tau = \Delta$  finite, we obtain the Schwinger-Keldysh generating function  $Z[\xi] = \text{Tr}[\rho(t_f, \{\xi\})]$  for a given quantum trajectory  $\{\xi_{ij}(t)\}$  and the corresponding action of Eq.(1).

The generating function  $Z[\xi]$  gives the Born probability of the quantum trajectory  $\{\xi_{ij}(t)\}$ , and the expectation value of any operator  $A$  in the long-time steady state is obtained as  $\langle A \rangle_\xi = (1/Z[\xi]) \int \mathcal{D}\theta A[\theta] e^{iS[\theta, \xi]/\hbar}$ . Further, the trajectory averaged expectation value,  $\overline{\langle A \rangle} = (1/Z) \int \mathcal{D}\xi Z[\xi] \langle A \rangle_\xi$ , can be obtained from the generating  $\mathcal{Z} = \int \mathcal{D}\xi Z[\xi]$ , which is equal to 1 due to normalization of the Born probability.

## Appendix B: Self-consistent harmonic approximation (SCHA) and effective action

For the SCHA, we take a harmonic variational action

$$\begin{aligned} S_v[\theta, \xi] &= \int_{t_0}^{t_f} dt \left[ \sum_{i,s} s \left\{ \frac{\hbar^2 \dot{\theta}_{is}^2}{2E_c} + \frac{\hbar^2 \gamma}{E_c} \dot{\theta}_{is} \sum_{j \in \text{nn}_i} \xi_{ij}(t) \right. \right. \\ &\quad \left. \left. - \sum_{\langle ij \rangle, s} s \left\{ \frac{1}{2} D_{ij,s}(t) \Delta\theta_{ij,s}^2 - \frac{is\hbar}{2\Delta} (\xi_{ij}(t) - \Delta\theta_{ij,s})^2 \right\} \right\} \right], \quad (\text{B1}) \end{aligned}$$

where  $D_{ij,s}(t)$  are the variational parameters and  $\text{nn}_i$  denotes the set of nearest neighbor sites of  $i$ . A variational principle can be obtained for the Born probability  $Z[\xi] = e^{-F[\xi]}$  as

$$Z[\xi] = Z_v[\xi] \langle e^{i(S-S_v)/\hbar} \rangle_v \geq Z_v[\xi] e^{i(S-S_v)_v/\hbar} \equiv e^{-F_v[\xi]}, \quad (\text{B2})$$

leading to  $F_v = -(i/\hbar) \langle S - S_v \rangle_v - \ln Z_v \geq F$ , where  $\langle \dots \rangle_v$  is expectation value with respect to the variational action. We obtain a self-consistency condition by minimizing  $F_v$  with respect to  $D_{ij,s}(t)$  (see Supplementary Sec.S2). Further, averaging over all the trajectories weighted with Born probability, and assuming a space-time translationally invariant steady state, i.e.,  $D_{ij,s}(t) = D$ , we obtain the self-consistency condition of Eq.(2). The expectation value,  $\overline{\langle \Delta\theta_{ij,s}^2(t) \rangle}_v = i(1/Nd) \sum_q K(\mathbf{q}) G^K(q)$ , in Eq.(2) is obtained using the trajectory averaged generating function  $\mathcal{Z} = \int \mathcal{D}\theta e^{iS_{\text{eff}}[\theta]/\hbar}$ , with the effective action  $S_{\text{eff}}$  of Eq.(3) (see Supplementary Sec.S21).

\* purnendudas@iisc.ac.in; sumilan@iisc.ac.in

<sup>1</sup> L. D. Landau and L. M. Lifshitz. *Quantum Mechanics Non-Relativistic Theory, Third Edition: Volume*

3. Butterworth-Heinemann, 3 edition, January 1981. ISBN 0750635398. URL <http://www.worldcat.org/isbn/0750635398>.

- <sup>2</sup> J. J. Sakurai and Jim Napolitano. *Modern Quantum Mechanics*. Cambridge University Press, 3 edition, 2020.
- <sup>3</sup> Howard M. Wiseman and Gerard J. Milburn. *Quantum Measurement and Control*. Cambridge University Press, 11 2009. ISBN 978-0-511-81394-8. doi: 10.1017/cbo9780511813948.
- <sup>4</sup> Brian Skinner, Jonathan Ruhman, and Adam Nahum. Measurement-induced phase transitions in the dynamics of entanglement. *Phys. Rev. X*, 9:031009, 2019. doi: 10.1103/PhysRevX.9.031009.
- <sup>5</sup> Soonwon Choi, Yimu Bao, Xiao-Liang Qi, and Ehud Altman. Quantum error correction in scrambling dynamics and measurement-induced phase transition. *Phys. Rev. Lett.*, 125:030505, 2020. doi: 10.1103/PhysRevLett.125.030505.
- <sup>6</sup> Chao-Ming Jian, Yi-Zhuang You, Romain Vasseur, and Andreas W. W. Ludwig. Measurement-induced criticality in random quantum circuits. *Phys. Rev. B*, 101:104302, 2020. doi:10.1103/PhysRevB.101.104302.
- <sup>7</sup> Yaodong Li, Xiao Chen, and Matthew P. A. Fisher. Measurement-driven entanglement transition in hybrid quantum circuits. *Phys. Rev. B*, 100:134306, 2019. doi: 10.1103/PhysRevB.100.134306.
- <sup>8</sup> Michael J. Gullans and David A. Huse. Dynamical purification phase transition induced by quantum measurements. *Phys. Rev. X*, 10:041020, 2020. doi: 10.1103/PhysRevX.10.041020.
- <sup>9</sup> O. Alberton, M. Buchhold, and S. Diehl. Entanglement transition in a monitored free-fermion chain: From extended criticality to area law. *Phys. Rev. Lett.*, 126:170602, Apr 2021. doi:10.1103/PhysRevLett.126.170602. URL <https://link.aps.org/doi/10.1103/PhysRevLett.126.170602>.
- <sup>10</sup> Yimu Bao, Soonwon Choi, and Ehud Altman. Theory of the phase transition in random unitary circuits with measurements. *Phys. Rev. B*, 101:104301, Mar 2020. doi: 10.1103/PhysRevB.101.104301. URL <https://link.aps.org/doi/10.1103/PhysRevB.101.104301>.
- <sup>11</sup> Shengqi Sang, Yaodong Li, Tianci Zhou, Xiao Chen, Timothy H. Hsieh, and Matthew P.A. Fisher. Entanglement negativity at measurement-induced criticality. *PRX Quantum*, 2:030313, Jul 2021. doi: 10.1103/PRXQuantum.2.030313. URL <https://link.aps.org/doi/10.1103/PRXQuantum.2.030313>.
- <sup>12</sup> Maxwell Block, Yimu Bao, Soonwon Choi, Ehud Altman, and Norman Y. Yao. Measurement-induced transition in long-range interacting quantum circuits. *Phys. Rev. Lett.*, 128:010604, Jan 2022. doi:10.1103/PhysRevLett.128.010604. URL <https://link.aps.org/doi/10.1103/PhysRevLett.128.010604>.
- <sup>13</sup> Igor Poboiko, Igor V. Gornyi, and Alexander D. Mirlin. Measurement-induced phase transition for free fermions above one dimension. *Phys. Rev. Lett.*, 132:110403, Mar 2024. doi:10.1103/PhysRevLett.132.110403. URL <https://link.aps.org/doi/10.1103/PhysRevLett.132.110403>.
- <sup>14</sup> Shao-Kai Jian, Chunxiao Liu, Xiao Chen, Brian Swingle, and Pengfei Zhang. Measurement-induced phase transition in the monitored sachdev-ye-kitaev model. *Phys. Rev. Lett.*, 127:140601, 2021. doi: 10.1103/PhysRevLett.127.140601.
- <sup>15</sup> Adam Nahum, Sthitadhi Roy, Brian Skinner, and Jonathan Ruhman. Measurement and entanglement phase transitions in all-to-all quantum circuits, on quantum trees, and in landau-ginsburg theory. *PRX Quantum*, 2:010352, 2021. doi:10.1103/PRXQuantum.2.010352.
- <sup>16</sup> Qicheng Tang and W. Zhu. Measurement-induced phase transition: A case study in the nonintegrable model by density-matrix renormalization group calculations. *Phys. Rev. Res.*, 2:013022, Jan 2020. doi: 10.1103/PhysRevResearch.2.013022. URL <https://link.aps.org/doi/10.1103/PhysRevResearch.2.013022>.
- <sup>17</sup> Richard F. Voss and Richard A. Webb. Phase coherence in a weakly coupled array of 20 000 nb josephson junctions. *Phys. Rev. B*, 25:3446–3449, Mar 1982. doi:10.1103/PhysRevB.25.3446. URL <https://link.aps.org/doi/10.1103/PhysRevB.25.3446>.
- <sup>18</sup> Richard A. Webb, Richard F. Voss, G. Grinstein, and P. M. Horn. Magnetic field behavior of a josephson-junction array: Two-dimensional flux transport on a periodic substrate. *Phys. Rev. Lett.*, 51:690–693, Aug 1983. doi: 10.1103/PhysRevLett.51.690. URL <https://link.aps.org/doi/10.1103/PhysRevLett.51.690>.
- <sup>19</sup> Gerd SchÄ¶n and A.D. Zaikin. Quantum coherent effects, phase transitions, and the dissipative dynamics of ultra small tunnel junctions. *Physics Reports*, 198(5):237–412, 1990. ISSN 0370-1573. doi:https://doi.org/10.1016/0370-1573(90)90156-V. URL <https://www.sciencedirect.com/science/article/pii/037015739090156V>.
- <sup>20</sup> Rosario Fazio and Herre van der Zant. Quantum phase transitions and vortex dynamics in superconducting networks. *Physics Reports*, 355(4):235–334, 2001. doi:10.1016/S0370-1573(01)00022-9. URL <https://www.sciencedirect.com/science/article/pii/S0370157301000229>.
- <sup>21</sup> S. L. Sondhi, S. M. Girvin, J. P. Carini, and D. Shahar. Continuous quantum phase transitions. *Rev. Mod. Phys.*, 69:315–333, Jan 1997. doi:10.1103/RevModPhys.69.315. URL <https://link.aps.org/doi/10.1103/RevModPhys.69.315>.
- <sup>22</sup> S. Sachdev. *Quantum phase transitions*. Cambridge University Press, Cambridge, second ed. edition, 2011. ISBN 9780521514682.
- <sup>23</sup> B. G. Orr, H. M. Jaeger, A. M. Goldman, and C. G. Kuper. Global phase coherence in two-dimensional granular superconductors. *Phys. Rev. Lett.*, 56:378–381, Jan 1986. doi:10.1103/PhysRevLett.56.378. URL <https://link.aps.org/doi/10.1103/PhysRevLett.56.378>.
- <sup>24</sup> H. M. Jaeger, D. B. Haviland, A. M. Goldman, and B. G. Orr. Threshold for superconductivity in ultrathin amorphous gallium films. *Phys. Rev. B*, 34:4920–4923, Oct 1986. doi:10.1103/PhysRevB.34.4920. URL <https://link.aps.org/doi/10.1103/PhysRevB.34.4920>.
- <sup>25</sup> John M. Martinis, Michel H. Devoret, and John Clarke. Experimental tests for the quantum behavior of a macroscopic degree of freedom: The phase difference across a josephson junction. *Phys. Rev. B*, 35:4682–4698, Apr 1987. doi:10.1103/PhysRevB.35.4682. URL <https://link.aps.org/doi/10.1103/PhysRevB.35.4682>.
- <sup>26</sup> D. B. Haviland, Y. Liu, and A. M. Goldman. Onset of superconductivity in the two-dimensional limit. *Phys. Rev. Lett.*, 62:2180–2183, May 1989. doi: 10.1103/PhysRevLett.62.2180. URL <https://link.aps.org/doi/10.1103/PhysRevLett.62.2180>.
- <sup>27</sup> Allen M. Goldman and Nina Markovic. Superconductor-insulator transitions in the two-dimensional limit. *Physics Today*, 51(11):39–44, 11 1998. ISSN 0031-9228. doi: 10.1063/1.882069. URL <https://doi.org/10.1063/1.882069>.

- <sup>28</sup> J. S. Penttilä, Ü. Parts, P. J. Hakonen, M. A. Paalanen, and E. B. Sonin. “superconductor-insulator transition” in a single josephson junction. *Phys. Rev. Lett.*, 82:1004–1007, Feb 1999. doi:10.1103/PhysRevLett.82.1004. URL <https://link.aps.org/doi/10.1103/PhysRevLett.82.1004>.
- <sup>29</sup> A. J. Rimberg, T. R. Ho, Ç. Kurdak, John Clarke, K. L. Campman, and A. C. Gossard. Dissipation-driven superconductor-insulator transition in a two-dimensional josephson-junction array. *Phys. Rev. Lett.*, 78:2632–2635, Mar 1997. doi:10.1103/PhysRevLett.78.2632. URL <https://link.aps.org/doi/10.1103/PhysRevLett.78.2632>.
- <sup>30</sup> Karl-Heinz Wagenblast, Anne van Otterlo, Gerd Schön, and Gergely T. Zimányi. Superconductor-insulator transition in a tunable dissipative environment. *Phys. Rev. Lett.*, 79:2730–2733, Oct 1997. doi:10.1103/PhysRevLett.79.2730. URL <https://link.aps.org/doi/10.1103/PhysRevLett.79.2730>.
- <sup>31</sup> Yamaguchi Takahide, Ryuta Yagi, Akinobu Kanda, Youiti Ootuka, and Shun-ichi Kobayashi. Superconductor-insulator transition in a two-dimensional array of resistively shunted small josephson junctions. *Phys. Rev. Lett.*, 85:1974–1977, Aug 2000. doi:10.1103/PhysRevLett.85.1974. URL <https://link.aps.org/doi/10.1103/PhysRevLett.85.1974>.
- <sup>32</sup> Albert Schmid. Diffusion and localization in a dissipative quantum system. *Phys. Rev. Lett.*, 51:1506–1509, Oct 1983. doi:10.1103/PhysRevLett.51.1506. URL <https://link.aps.org/doi/10.1103/PhysRevLett.51.1506>.
- <sup>33</sup> Sudip Chakravarty, Gert-Ludwig Ingold, Steven Kivelson, and Alan Luther. Onset of global phase coherence in josephson-junction arrays: A dissipative phase transition. *Phys. Rev. Lett.*, 56:2303–2306, 1986. doi:10.1103/PhysRevLett.56.2303.
- <sup>34</sup> Sudip Chakravarty, Gert-Ludwig Ingold, Steven Kivelson, and Gergely Zimanyi. Quantum statistical mechanics of an array of resistively shunted josephson junctions. *Phys. Rev. B*, 37:3283–3294, 1988. doi:10.1103/PhysRevB.37.3283.
- <sup>35</sup> Arno Kampf and Gerd Schön. Quantum effects and the dissipation by quasiparticle tunneling in arrays of josephson junctions. *Phys. Rev. B*, 36:3651–3660, 1987. doi:10.1103/PhysRevB.36.3651.
- <sup>36</sup> Luca Capriotti, Alessandro Cuccoli, Andrea Fubini, Valerio Tognetti, and Ruggero Vaia. Dissipation-driven phase transition in two-dimensional josephson arrays. *Phys. Rev. Lett.*, 94:157001, Apr 2005. doi:10.1103/PhysRevLett.94.157001. URL <https://link.aps.org/doi/10.1103/PhysRevLett.94.157001>.
- <sup>37</sup> Lukas M. Sieberer, Michael Buchhold, Jamir Marino, and Sebastian Diehl. Universality in driven open quantum matter. *arXiv e-prints*, art. arXiv:2312.03073, December 2023. doi:10.48550/arXiv.2312.03073.
- <sup>38</sup> S. Diehl, A. Micheli, A. Kantian, B. Kraus, H. P. Bächteler, and P. Zoller. Quantum states and phases in driven open quantum systems with cold atoms. *Nature Physics*, 4(11):878–883, November 2008. doi:10.1038/nphys1073. URL <https://doi.org/10.1038/nphys1073>.
- <sup>39</sup> S. Diehl, W. Yi, A. J. Daley, and P. Zoller. Dissipation-induced  $d$ -wave pairing of fermionic atoms in an optical lattice. *Phys. Rev. Lett.*, 105:227001, Nov 2010. doi:10.1103/PhysRevLett.105.227001. URL <https://link.aps.org/doi/10.1103/PhysRevLett.105.227001>.
- <sup>40</sup> Sebastian Diehl, Andrea Tomadin, Andrea Micheli, Rosario Fazio, and Peter Zoller. Dynamical phase transitions and instabilities in open atomic many-body systems. *Phys. Rev. Lett.*, 105:015702, Jul 2010. doi:10.1103/PhysRevLett.105.015702. URL <https://link.aps.org/doi/10.1103/PhysRevLett.105.015702>.
- <sup>41</sup> Sebastian Diehl, Enrique Rico, Mikhail A. Baranov, and Peter Zoller. Topology by dissipation in atomic quantum wires. *Nature Physics*, 7(12):971–977, December 2011. doi:10.1038/nphys2106. URL <https://doi.org/10.1038/nphys2106>.
- <sup>42</sup> Andrea Tomadin, Sebastian Diehl, and Peter Zoller. Nonequilibrium phase diagram of a driven and dissipative many-body system. *Phys. Rev. A*, 83:013611, Jan 2011. doi:10.1103/PhysRevA.83.013611. URL <https://link.aps.org/doi/10.1103/PhysRevA.83.013611>.
- <sup>43</sup> A. Tomadin, S. Diehl, M. D. Lukin, P. Rabl, and P. Zoller. Reservoir engineering and dynamical phase transitions in optomechanical arrays. *Phys. Rev. A*, 86:033821, Sep 2012. doi:10.1103/PhysRevA.86.033821. URL <https://link.aps.org/doi/10.1103/PhysRevA.86.033821>.
- <sup>44</sup> L. M. Sieberer, S. D. Huber, E. Altman, and S. Diehl. Dynamical critical phenomena in driven-dissipative systems. *Phys. Rev. Lett.*, 110:195301, May 2013. doi:10.1103/PhysRevLett.110.195301. URL <https://link.aps.org/doi/10.1103/PhysRevLett.110.195301>.
- <sup>45</sup> Jamir Marino and Sebastian Diehl. Driven markovian quantum criticality. *Phys. Rev. Lett.*, 116:070407, Feb 2016. doi:10.1103/PhysRevLett.116.070407. URL <https://link.aps.org/doi/10.1103/PhysRevLett.116.070407>.
- <sup>46</sup> Michael Buchhold, Benjamin Everest, Matteo Marcuzzi, Igor Lesanovsky, and Sebastian Diehl. Nonequilibrium effective field theory for absorbing state phase transitions in driven open quantum spin systems. *Phys. Rev. B*, 95:014308, Jan 2017. doi:10.1103/PhysRevB.95.014308. URL <https://link.aps.org/doi/10.1103/PhysRevB.95.014308>.
- <sup>47</sup> Steven Mathey and Sebastian Diehl. Dynamic renormalization group theory for open floquet systems. *Phys. Rev. B*, 102:134307, Oct 2020. doi:10.1103/PhysRevB.102.134307. URL <https://link.aps.org/doi/10.1103/PhysRevB.102.134307>.
- <sup>48</sup> Carlton M. Caves and G. J. Milburn. Quantum-mechanical model for continuous position measurements. *Phys. Rev. A*, 36:5543–5555, 1987. doi:10.1103/PhysRevA.36.5543.
- <sup>49</sup> M. I. Dykman, M. Marthaler, and V. Peano. Quantum heating of a parametrically modulated oscillator: Spectral signatures. *Phys. Rev. A*, 83:052115, May 2011. doi:10.1103/PhysRevA.83.052115. URL <https://link.aps.org/doi/10.1103/PhysRevA.83.052115>.
- <sup>50</sup> Alex Kamenev. *Field theory of non-equilibrium systems*. Cambridge University Press, 2011.
- <sup>51</sup> Sibaram Ruidas and Sumilan Banerjee. Semiclassical limit of a measurement-induced transition in many-body chaos in integrable and nonintegrable oscillator chains. *Phys. Rev. Lett.*, 132:030402, 2024. doi:10.1103/PhysRevLett.132.030402.
- <sup>52</sup> Chakraverty, B.K. Possibility of insulator to superconductor phase transition. *J. Physique Lett.*, 40(5):99–100, 1979. doi:10.1051/jphyslet:0197900400509900. URL <https://doi.org/10.1051/jphyslet:0197900400509900>.
- <sup>53</sup> E. Šimánek. Instability of granular superconductivity. *Phys. Rev. B*, 22:459–462, Jul 1980. doi:10.1103/PhysRevB.22.459. URL <https://link.aps.org/doi/10.1103/PhysRevB.22.459>.
- <sup>54</sup> V. L. Berezinsky. Destruction of long range order in one-dimensional and two-dimensional systems having a con-



tinuous symmetry group. I. Classical systems. *Sov. Phys. JETP*, 32:493–500, 1971.

- <sup>55</sup> J M Kosterlitz and D J Thouless. Ordering, metastability and phase transitions in two-dimensional systems. *Journal of Physics C: Solid State Physics*, 6(7):1181, apr 1973. doi: 10.1088/0022-3719/6/7/010. URL <https://dx.doi.org/10.1088/0022-3719/6/7/010>.
- <sup>56</sup> A. O. Caldeira and A. J. Leggett. Influence of dissipation on quantum tunneling in macroscopic systems. *Phys. Rev. Lett.*, 46:211–214, Jan 1981. doi: 10.1103/PhysRevLett.46.211. URL <https://link.aps.org/doi/10.1103/PhysRevLett.46.211>.

**Supplemental Material  
for**

**Superconductor-Insulator Transition in Weakly Monitored Josephson Junction Arrays**

Purnendu Das<sup>1</sup>, Sumilan Banerjee<sup>2</sup>

<sup>1</sup>Department of Physics, Indian Institute of Science, Bangalore 560012, India

<sup>2</sup>Centre for Condensed Matter Theory, Department of Physics, Indian Institute of Science, Bangalore 560012, India

**S1: Schwinger-Keldysh (SK) path integral for monitored Josephson junction arrays (JJA)**

In this section, we briefly discuss the path integral representations of  $Z[\xi] = \text{Tr}[\rho(\{\xi\}, t_f)]$  for the density matrix evolution of Eq.(A2) in the continuous weak measurement limit  $\sigma \rightarrow \infty$ ,  $\tau \rightarrow 0$  with  $\sigma\tau = \Delta$  finite. In this limit, we get

$$Z[\xi] = \int_{\theta_{\pm}(t_f)=\theta(t_f)} \prod_i d\theta_i(t_f) \prod_{s=\pm 1, n=0}^{M-1} d\theta_{is}(t_0 + n\tau) \langle \theta_+(t_0) | \rho_0 | \theta_-(t_0) \rangle$$

$$\prod_{t=t_0}^{t_f-\tau} \left\langle \theta_+(t+\tau) \left| e^{i\gamma\tau \sum_{\langle ij \rangle} \xi_{ij}(t+\tau)(\hat{n}_i - \hat{n}_j)} e^{-\tau \sum_{\langle ij \rangle} [\xi_{ij}(t+\tau) - (\hat{\theta}_i - \hat{\theta}_j)]^2 / 2\Delta} e^{-iH_{s\tau}/\hbar} \right| \theta_+(t) \right\rangle \quad (\text{S1.1})$$

$$\prod_{t=t_0}^{t_f-\tau} \langle \theta_-(t+\tau) \left| e^{i\gamma\tau \sum_{\langle ij \rangle} \xi_{ij}(t+\tau)(\hat{n}_i - \hat{n}_j)} e^{-\tau \sum_{\langle ij \rangle} [\xi_{ij}(t+\tau) - (\hat{\theta}_i - \hat{\theta}_j)]^2 / 2\Delta} e^{-iH_{s\tau}/\hbar} \right| \theta_-(t) \rangle^*,$$

where the matrix elements above can be evaluated as,

$$\langle \theta(t+\tau) \left| e^{i\gamma\tau \sum_{\langle ij \rangle} \xi_{ij}(t+\tau)(\hat{n}_i - \hat{n}_j)} e^{-\tau \sum_{\langle ij \rangle} [\xi_{ij}(t+\tau) - (\hat{\theta}_i - \hat{\theta}_j)]^2 / 2\Delta} e^{-iH_{s\tau}/\hbar} \right| \theta(t) \rangle$$

$$\sim e^{\frac{i\hbar}{2E_c\tau} \sum_i [\theta_i(t+\tau) - \theta_i(t) + \gamma\tau \tilde{\xi}_i(t+\tau)]^2} e^{-\frac{i\tau}{\hbar} \sum_{\langle ij \rangle} J_{ij} [1 - \cos(\theta_i(t) - \theta_j(t))]} e^{-\frac{\tau}{2\Delta} \sum_{\langle ij \rangle} [\xi_{ij}(t+\tau) - \{\theta_i(t+\tau) - \theta_j(t+\tau) - \gamma\tau(\tilde{\xi}_i(t+\tau) - \tilde{\xi}_j(t+\tau))\}]^2}$$

(S1.2)

where  $\tilde{\xi}_i = \sum_{j \in \text{nn}_i} \xi_{ij}$  with  $\xi_{ji} = -\xi_{ij}$ . In the above, we do not explicitly include the pre-factor as it cancels between numerator and denominator while calculating expectation value of any observable using the generating function  $Z[\xi]$ . In the continuum limit,  $\tau \rightarrow 0$ , we obtain

$$Z[\xi] = \int_{\theta_{\pm}(t_f)=\theta(t_f)} \prod_i d\theta_i(t_f) \prod_{s,n=0}^{M-1} d\theta_{is}(t_0 + n\tau) \langle \theta_+(t_0) | \rho_0 | \theta_-(t_0) \rangle$$

$$\prod_{t=t_0, s}^{t_f-\tau} e^{\frac{i\hbar\tau}{2E_c} \sum_{i,s} s [\dot{\theta}_{is}(t)^2 + 2\dot{\theta}_{is}(t)\gamma\tilde{\xi}_i(t^+) - \frac{i\tau}{\hbar} \sum_{\langle ij \rangle, s} s J_{ij} [1 - \cos(\theta_{is}(t) - \theta_{js}(t))]} e^{-\frac{\tau}{2\Delta} \sum_{\langle ij \rangle} [\xi_{ij}(t^+) - (\theta_{is}(t^+) - \theta_{is}(t^+))]^2} \quad (\text{S1.3})$$

$$= \int \mathcal{D}\theta e^{iS[\theta, \xi]/\hbar} \langle \theta_+(t_0) | \rho_0 | \theta_-(t_0) \rangle$$

The above is a path integral on the SK contour of Fig.2(a) with the action in Eq.(1) (main text). Further, for long-time steady state, we take  $t_0 \rightarrow -\infty$  and  $t_f \rightarrow \infty$ .

**S2: Variational principle and self-consistent harmonic approximation (SCHA) for the dynamics of monitored JJA**

Here we discuss a variational principle for the Born probability  $Z[\xi] = e^{-F[\xi]}$  of a quantum trajectory and its application in terms of a SCHA, as mentioned in the main text and in Appendix B. The Born probability  $Z[\xi] = \int \mathcal{D}\theta e^{iS[\theta, \xi]}$  can be expressed in terms of a variational action  $S_v[\theta, \xi]$  and corresponding partition function  $Z_v = \int \mathcal{D}\theta e^{iS_v[\theta, \xi]}$  by the following expression,

$$Z = Z_v \left[ \frac{1}{Z_v} \int \mathcal{D}\theta e^{i(S - S_v)/\hbar} e^{iS_v/\hbar} \right] = Z_v \left\langle e^{i(S - S_v)/\hbar} \right\rangle_v \quad (\text{S2.1})$$

Using the identity  $\langle e^A \rangle \geq e^{\langle A \rangle}$  we can write  $Z \geq Z_v e^{i\langle S - S_v \rangle_v / \hbar}$ . As a result,

$$F[\xi] \leq -\log Z_v - i\langle S - S_v \rangle_v / \hbar = F_v \quad (\text{S2.2})$$

To obtain self-consistent equation, we minimize the  $F_v[\xi]$  with respect to the variational parameter  $D_{ij,s}(t)$  in the variational action of Eq.(B1) and get

$$\int_{-\infty}^{\infty} dt \sum_{\langle ij \rangle, s} s [J \frac{\partial}{\partial D_{ij,s}(t)} [1 - \langle \cos(\theta_{is}(t) - \theta_{js}(t)) \rangle_v] - \frac{D_{ij,s}(t)}{2} \frac{\partial}{\partial D_{ij,s}(t)} \langle (\theta_{is}(t) - \theta_{js}(t))^2 \rangle_v] = 0 \quad (\text{S2.3})$$

To further solve the above equation, we perform a trajectory averaging, assuming a long-time steady state with space-time translation invariance, i.e.,  $D_{ij,s}(t) = D$ , leading to

$$J \frac{\partial}{\partial D} \overline{\langle \cos(\Delta\theta_{ij,s}(t)) \rangle_v} + \frac{D}{2} \frac{\partial}{\partial D} \overline{\langle (\Delta\theta_{ij,s}(t))^2 \rangle_v} = 0. \quad (\text{S2.4})$$

Where,

$$\overline{\langle \cos[\Delta\theta_{ij,s}(t)] \rangle_v} = \frac{1}{\mathcal{Z}} \text{Re} \int \mathcal{D}\theta e^{iS_{eff}[\theta]} e^{i(\theta_{is}(t) - \theta_{js}(t))} \quad (\text{S2.5})$$

for the effective action of Eq.(3). To this end,

$$iS_{eff}/\hbar + i(\theta_{ks}(t) - \theta_{ls}(t)) = \frac{i}{2\hbar} \int_{-\infty}^{\infty} dt \sum_{ij} [\theta_{ic}(t) \ \theta_{iq}(t)] \begin{bmatrix} G_{ij,cc}^{-1}(\xi_{ij}, t, t') & G_{ij,cq}^{-1}(\xi_{ij}, t, t') \\ G_{ij,qc}^{-1}(\xi_{ij}, t, t') & G_{ij,qq}^{-1}(\xi_{ij}, t, t') \end{bmatrix} \begin{bmatrix} \theta_{ic}(t') \\ \theta_{iq}(t') \end{bmatrix} \quad (\text{S2.6})$$

$$+ i \sum_i \int_{-\infty}^{\infty} dt' [\theta_{ic}(t) \ \theta_{iq}(t)] \begin{bmatrix} (\delta_{ik} - \delta_{il})\delta(t - t') \\ s(\delta_{ik} - \delta_{il})\delta(t - t') \end{bmatrix}, \quad (\text{S2.7})$$

where we have performed the Keldysh rotation<sup>50</sup>  $\theta_{is}(t) = \theta_{ic}(t) + s\theta_{iq}(t)$ , and the propagators  $G_{ij,\alpha\beta}^{-1}$  ( $\alpha, \beta = c, q$ ) are given in the main text below Eq.(3). Using the above and performing the Gaussian integrals in Eq.(S2.5), we obtain

$$\overline{\langle \cos(\theta_{ks}(t) - \theta_{ls}(t)) \rangle_v} = \exp \left( -\frac{i}{2} \sum_{ij} [(\delta_{ik} - \delta_{il}) \ s(\delta_{jk} - \delta_{jl})] \begin{bmatrix} G_{ij,cc} & G_{ij,cq} \\ G_{ij,qc} & G_{ij,qq} \end{bmatrix} \begin{bmatrix} (\delta_{ik} - \delta_{il}) \\ s(\delta_{ik} - \delta_{il}) \end{bmatrix} \right) \quad (\text{S2.8})$$

$$= \exp \left( -\frac{1}{2} i \sum_{ij} (\delta_{ik} - \delta_{il})(\delta_{jk} - \delta_{jl})(G_{ij,cc} + G_{ij,cq} + G_{ij,qc} + G_{ij,qq})(t, t) \right) \quad (\text{S2.9})$$

$$(\text{S2.10})$$

It is straightforward to show that for the Gaussian action of Eq.(3),

$$\overline{\langle (\theta_{ks}(t) - \theta_{ls}(t))^2 \rangle_v} = i \sum_{ij} (\delta_{ik} - \delta_{il})(\delta_{jk} - \delta_{jl})(G_{ij,cc} + G_{ij,cq} + G_{ij,qc} + G_{ij,qq})(t, t). \quad (\text{S2.11})$$

Hence,

$$\overline{\langle \cos(\theta_{ks}(t) - \theta_{ls}(t)) \rangle_v} = \exp \left( -\frac{1}{2} \overline{\langle (\theta_{ks}(t) - \theta_{ls}(t))^2 \rangle_v} \right) \quad (\text{S2.12})$$

Thus, we get

$$\frac{\partial}{\partial D} \overline{\langle \cos(\Delta\theta_{ij,s}(t)) \rangle_v} = \frac{1}{2} \overline{\langle \cos(\Delta\theta_{ij,s}(t)) \rangle_v} \frac{\partial}{\partial D} \overline{\langle (\Delta\theta_{ij,s}(t))^2 \rangle_v} \quad (\text{S2.13})$$

Using Eq.(S2.4), the above leads to the self-consistency condition of Eq.(2) (main text).

### 1. Effective action for SCHA

To obtain the effective action of Eq.(3) for the trajectory averaged generating function  $\mathcal{Z} = \int \mathcal{D}\theta e^{iS_{eff}[\theta]}$ , we first integrate out the measurement outcomes  $\{\xi_{ij}(t)\}$ ,

$$\begin{aligned} & \int \mathcal{D}\xi e^{-\int_{-\infty}^{\infty} dt [\frac{1}{\Delta} \sum_{\langle ij \rangle} \xi_{ij}^2 + \frac{2i}{\hbar} \sum_i \theta_{ic} \frac{i\hbar}{\Delta} \tilde{\xi}_i + \frac{2i}{\hbar} \sum_i \theta_{iq} m\gamma \partial_t \tilde{\xi}_i]} \\ &= \exp \left\{ \frac{i}{\hbar} \int_{-\infty}^{\infty} dt \sum_{ij} [\theta_{ic}(t) \ \theta_{iq}(t)] \begin{bmatrix} -i\frac{\hbar}{\Delta} K_{ij} & -i\frac{\hbar^2\gamma}{E_c} K_{ij}(i\partial_t - i\eta) \\ i\frac{\hbar^2\gamma}{E_c} K_{ij}(i\partial_t + i\eta) & -i\frac{\hbar^3\gamma^2}{E_c^2\Delta^{-1}} K_{ij}\partial_t^2 \end{bmatrix} \begin{bmatrix} \theta_{jc}(t) \\ \theta_{jq}(t) \end{bmatrix} \right\} \end{aligned} \quad (\text{S2.14})$$

The above leads to the effective Gaussian action for SCHA,

$$\begin{aligned} S_{eff} &= \int_{-\infty}^{\infty} dt \sum_{ij} [\theta_{ic}(t) \ \theta_{iq}(t)] \\ & \begin{bmatrix} 0 & \frac{\hbar^2}{E_c} (i\partial_t - i\eta)^2 \delta_{ij} - [D_{ij,c}(t) + i\frac{\hbar^2\gamma}{E_c} (i\partial_t - i\eta)] K_{ij} \\ \frac{\hbar^2}{E_c} (i\partial_t + i\eta)^2 \delta_{ij} - [D_{ij,c}(t) - i\frac{\hbar^2\gamma}{E_c} (i\partial_t + i\eta)] K_{ij} & iK_{ij} (\frac{\hbar}{\Delta} - \frac{\hbar^3\gamma^2}{E_c^2\Delta^{-1}} \partial_t^2) \end{bmatrix} \begin{bmatrix} \theta_{ic}(t) \\ \theta_{iq}(t) \end{bmatrix} \end{aligned} \quad (\text{S2.15})$$

For the space-time translationally invariant steady state, assuming  $D_{ij,+}(t) = D_{ij,-}(t) = D$ , and Fourier transforming to momentum and frequency space, we obtain the action of Eq.(3) (main text).

By inverting the inverse propagator appearing in  $S_{eff}$  of Eq.(3), we obtain the SCHA propagator which has the usual causal structure<sup>50</sup>,

$$G(\mathbf{q}, \omega) = \begin{bmatrix} G^K(\mathbf{q}, \omega) & G^R(\mathbf{q}, \omega) \\ G^A(\mathbf{q}, \omega) & 0 \end{bmatrix} \quad (\text{S2.16})$$

$$G^R(\mathbf{q}, \omega) = \frac{\hbar}{2} \frac{1}{\hbar^2(\omega + i\eta)^2/E_c - [D - i\hbar^2\gamma(\omega + i\eta)/E_c]K(\mathbf{q})} \quad (\text{S2.17})$$

$$G^A(\mathbf{q}, \omega) = \frac{\hbar}{2} \frac{1}{\hbar^2(\omega - i\eta)^2/E_c - [D + i\hbar^2\gamma(\omega - i\eta)/E_c]K(\mathbf{q})} \quad (\text{S2.18})$$

$$G^K(\mathbf{q}, \omega) = \frac{E_c^2}{2\hbar^3} \left[ -iK(\mathbf{q}) \left( \frac{\hbar}{\Delta} + \frac{\hbar^3\gamma^2}{E_c^2\Delta^{-1}} \omega^2 \right) \right] \frac{1}{(\omega^2 - \omega_{\mathbf{q}}^2)^2 + \gamma^2 K(\mathbf{q})^2 \omega^2} \quad (\text{S2.19})$$

Here  $\omega_{\mathbf{q}}^2 = (E_c/\hbar^2)DK(\mathbf{q})$ . Using the above propagators we obtain

$$\begin{aligned} \overline{\langle \Delta\theta_{ij,s}^2(t) \rangle}_v &= \frac{E_c^2}{2\hbar^3 Nd} \sum_{\mathbf{q}} \int_{-\infty}^{\infty} \frac{d\omega}{2\pi} K^2(\mathbf{q}) \left( \frac{\hbar}{\Delta} + \frac{\hbar^3\gamma^2}{E_c^2\Delta^{-1}} \omega^2 \right) \frac{1}{(\omega^2 - \omega_{\mathbf{q}}^2)^2 + \gamma^2 K(\mathbf{q})^2 \omega^2} \\ &= \frac{E_c}{4dD} \frac{\Delta^{-1}}{\gamma} + \frac{\gamma}{2\Delta^{-1}} \end{aligned} \quad (\text{S2.21})$$

The above is used in Eq.(2) (main text) to compute the superfluid stiffness  $D$  self-consistently and to obtain the SCHA phase diagrams, discussed in the main text.

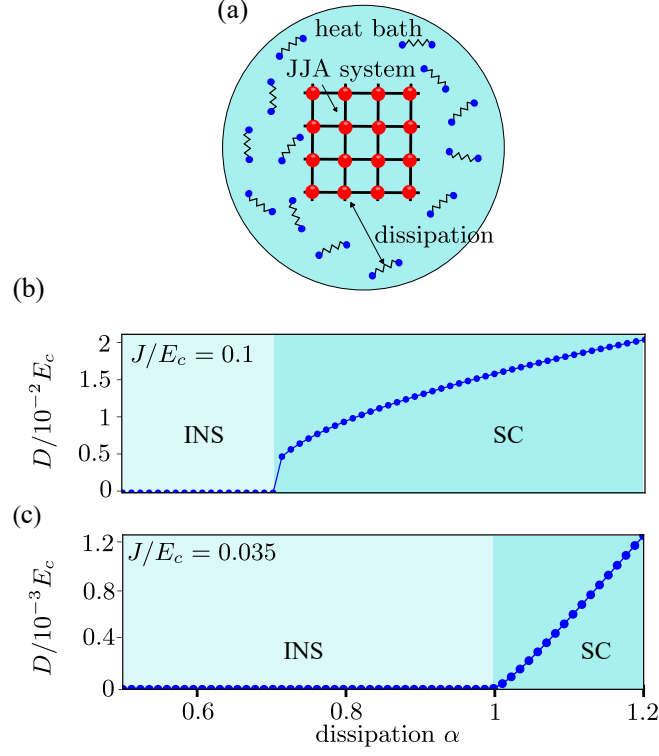


FIG. S1. **Ohmic JJA**:(a) The schematic diagram of a JJA coupled to an equilibrium Ohmic heat bath at constant temperatures  $T$  is shown. Red circles denote the superconducting island and the black lines represent the Josephson junctions. Heat bath degrees of freedom are depicted as oscillators. (b) A horizontal cut through  $J/E_c = 0.1$  is taken in Fig.1(c) (main text) for  $d = 1$ . We can see a jump in the value of  $D$  at the first-order transition within SCHA. (c) A horizontal cut through  $J/E_c = 0.035$  is taken in Fig.1(d) (main text). We can see a continuous phase transition at  $\alpha = 1/d$ .

### S3: Josephson junction arrays with Ohmic dissipation

In this section, we discuss the well-studied case<sup>33,34</sup> of JJA in contact with an external equilibrium Ohmic bath at a fixed temperature  $T$ . The bath is modeled by harmonic oscillators<sup>56</sup> as shown in Fig. 2 (a), and the combined system of the JJA on a hypercubic lattice in  $d$  dimension and the bath is described by the Hamiltonian,

$$H = H_s + H_b + H_{sb} \quad (\text{S3.1a})$$

$$H_s = \frac{1}{2} \sum_i E_c \hat{n}_i^2 + J \sum_{\langle ij \rangle} (1 - \cos(\hat{\theta}_i - \hat{\theta}_j)) \quad (\text{S3.1b})$$

$$H_b = \frac{1}{2} \sum_{\langle ij \rangle} \sum_l \left( \frac{\hat{p}_{l,ij}^2}{m_l} + m_l^2 \omega_l^2 \hat{x}_{l,ij}^2 \right) \quad (\text{S3.1c})$$

$$H_{sb} = \sum_{\langle ij \rangle} \Delta \hat{\theta}_{ij} \sum_l f_{l,ij} \hat{x}_{l,ij} \quad (\text{S3.1d})$$

where  $f_{l,ij}$  are the coupling parameters between phase difference and the bath oscillators with position  $\hat{x}_{l,ij}$ , momenta  $\hat{p}_{l,ij}$  and masses  $m_l$ .

We employ the Schwinger-Keldysh (SK) path integral method<sup>50</sup> for our analysis, as in the case monitored JJA. The SK generating function for the unitary evolution up to time  $t_f$  of the combined JJA and bath system starting from a density matrix  $\rho(t_0)$  at time  $t_0$  is written as a path integral

$$Z(t_f) = \text{Tr}[\rho(t_f)] = \text{Tr}[U(t_f, t_0)\rho(t_0)U(t_0, t_f)] = \int \mathcal{D}x \mathcal{D}\theta e^{i(S_s[\theta] + S_b[x] + S_{sb}[\theta, x])/\hbar}, \quad (\text{S3.2})$$

where  $U(t_f, t_0) = e^{iH(t_f - t_0)/\hbar}$ . It is straightforward to obtain the actions  $S_s[\theta]$ ,  $S_b[x]$  and  $S_{sb}[\theta, x]$  from the Hamiltonian of Eqs.(S3.1). We further integrate out the harmonic bath variables to obtain  $Z = \int \mathcal{D}\theta e^{iS[\theta]/\hbar}$  with an effective

action  $S[\theta]$  and assume usual Ohmic bath spectral function<sup>20,33,34,50</sup>.

### 1. Self-consistent harmonic approximation for Ohmic JJA

Following Refs.33 and 34, and as done for monitored JJA, we apply SCHA, where a variational action  $S_v[\theta]$  is written by replacing  $J(1 - \cos(\theta_i - \theta_j))$  in  $S[\theta]$  by the harmonic term  $(1/2)D(\theta_i - \theta_j)^2$  where  $D_{ij}$  is the variational parameter. Following procedure similar to the case of monitored JJA in Sec.S2, we get the following self-consistency condition<sup>33</sup>,

$$D = J \exp\left(-\frac{1}{2}\langle(\theta_i - \theta_j)^2\rangle_v\right). \quad (\text{S3.3})$$

Within SCHA, the action can be written as

$$\frac{1}{\hbar}S_v = \frac{1}{2} \sum_q \theta^T(-q)G^{-1}(q)\theta(q), \quad (\text{S3.4})$$

in terms of Fourier transform  $\theta^T(q) = (\phi_c(q), \phi_q(q))$  of the classical and quantum components of phase fields  $\theta_{is}(t) = \theta_{ic}(t) + s\theta_{iq}(t)$ , with  $q = (\mathbf{q}, \omega)$  and  $\sum_q = \sum_{\mathbf{q}} \int (d\omega/2\pi)$ . The inverse propagators are

$$[G^{-1}]^{R(A)}(q) = \frac{2}{\hbar} \left[ \frac{\hbar^2}{E_c} ((\omega \pm i\eta)^2 - \omega_{\mathbf{q}}^2) \pm \frac{\alpha\hbar\omega}{2\pi} K(\mathbf{q}) \right] \quad (\text{S3.5a})$$

$$[G^{-1}]^K(q) = \cot\left(\frac{\hbar\omega}{2T}\right) ([G^{-1}]^R(q) - [G^{-1}]^A(q)), \quad (\text{S3.5b})$$

Here we impose FDR on the Keldysh component for thermal equilibrium at temperature  $T$  ( $k_B = 1$ ). The dimensionless parameter  $\alpha = h/4e^2R$ , where  $R$  is the normal state resistance, controls the strength of dissipation. Using the variational action, we obtain

$$\langle\Delta\theta_{ij}^2\rangle_v = \frac{\hbar}{2Nd} \sum_{\mathbf{q}} \int_{-\infty}^{\infty} \frac{d\omega}{2\pi} K(\mathbf{q}) \coth\left(\frac{\hbar\omega}{2T}\right) \left( \frac{2\hbar\omega \frac{\alpha}{2\pi} K(\mathbf{q})}{\frac{\hbar^4}{E_c^2} (\omega^2 - \omega_{\mathbf{q}}^2)^2 + \hbar^2\omega^2 \frac{\alpha^2}{4\pi^2} K^2(\mathbf{q})} \right) \quad (\text{S3.6})$$

We reproduce the phase diagram of Refs.33 and 34 for Ohmic JJA by solving Eq.(S3.3) self-consistently using Eq.(S3.6) self-consistently within the Debye approximation  $K(q) \sim q^2$ , as shown in Fig.1(c,e) (main text). The line depicts the phase boundary between the insulating normal state and the superconducting state. The superfluid stiffness  $D$  (color) changes discontinuously across the solid line, as shown in Fig.S1(c) for  $J/E_c = 0.1$ , whereas  $D$  changes continuously across the dashed line, as shown in Fig.S1(d) for  $J/E_c = 0.035$ . The vertical boundary at  $\alpha = 1/d$  is a line of continuous transition. For  $\alpha < 1/d$  the quantum fluctuations destroy the long-range phase coherence even at  $T = 0$  for  $J/E_c$  below a critical value that varies with  $\alpha$ . From Fig.1(c) (main text), it is evident that for  $J/E_c$  values below a threshold, the phase transition is insensitive to  $J/E_c$ , depending only on  $\alpha$ . Thus, the transition is solely governed by dissipation parameter  $\alpha$  and beyond the critical value  $\alpha = 1/d$ , quantum fluctuations of Cooper pair number are entirely suppressed by dissipation, always leading to a phase coherent superconducting state at  $T = 0$ . We show the phase diagram in  $T - J$  plane in Fig.1 (e) (main text) for a fixed  $\alpha = 0.4$ . Here, the critical value of  $J/E_c$  increases with temperature, as expected due to the increase of thermal fluctuations with temperature. Qualitatively similar phase diagrams are obtained within SCHA for higher dimensions<sup>33,34</sup>.

We now compare the Ohmic JJA at high temperatures with monitored JJA within SCHA. At high temperature  $T$ , we expand  $\cot(\hbar\omega/2T)$  appearing in Eq.(S3.6) up to  $\mathcal{O}(\hbar\omega/T)$  to get,

$$\langle\Delta\theta_{ij}^2\rangle_{\text{var}} = \frac{1}{2Nd} \sum_{\mathbf{q}} \int_{-\infty}^{\infty} \frac{hd\omega}{2\pi} \left(1 + \frac{\hbar^2\omega^2}{12T^2}\right) \left( \frac{4T \frac{\alpha}{2\pi} K^2(\mathbf{q})}{\frac{\hbar^4}{E_c^2} (\omega^2 - \omega_{\mathbf{q}}^2)^2 + \hbar^2\omega^2 \frac{\alpha^2}{4\pi^2} K^2(\mathbf{q})} \right) \quad (\text{S3.7})$$

By comparing Eq.(S2.21) and Eq.(S3.7), we see the similarities between Ohmic and monitored JJAs, namely  $\hbar\gamma/E_c \sim \alpha/2\pi$  and  $\hbar\Delta^{-1}/E_c \sim 4\gamma T$ . Hence, the feedback strength of monitored JJA  $\gamma$  is equivalent to dissipation strength  $\alpha$  in the Ohmic JJA. Additionally, the measurement strength  $\Delta^{-1}$  exhibits behavior akin to the effective temperature  $T_{eff}$  (see main text) when  $\gamma$  is held constant, resembling the equilibrium temperature  $T$  of the Ohmic JJA.

#### S4: Discussion on the phase diagram of monitored JJA

We show the phase diagram of the monitored JJA in Figs.1(b,d), in the  $J - \gamma$  and  $T_{eff} - J$  planes, and in Fig.2(b) for  $J - \Delta^{-1}$ . The phase diagrams are numerically obtained from the self-consistent solution of Eq.(2) (main text) for  $d = 1$ . We observe that below a certain threshold value of  $J/E_c$ , the system remains insulating for any value of  $\gamma$ ,  $T_{eff}$  and  $\Delta^{-1}$ . Above the threshold  $J/E_c$ , the system undergoes a re-entrant insulator-superconductor-insulator transition as a function of  $\gamma$ ,  $T_{eff}$  and  $\Delta^{-1}$ . For the re-entrant phase transition observed in Fig.2(b), there is a significant jump in the observed value of superconducting stiffness  $D$  across the first transition and a smaller jump at the second transition (see Fig.2(c,d)).

We can gain analytical insights into the numerically obtained phase diagram. For any finite feedback  $\gamma$ , we get the self-consistent condition,  $D/E_c = (J/E_c) \exp(-\Delta^{-1}E_c/8d\gamma D - \gamma/4\Delta^{-1})$ . This condition can be expressed as,  $f(D) = \ln(D/E_c) + \Delta^{-1}E_c/8d\gamma D = \ln(J/E_c) - \gamma/4\Delta^{-1}$ . For a fixed value of  $\gamma$  and  $\Delta^{-1}$ , the minimum of  $f(D)$  reveals the discontinuity in  $D$  at the critical point, indicating a first-order phase transition within the SCHA, with the discontinuity given by,

$$D_c/E_c = \frac{\Delta^{-1}}{8d\gamma} \quad (\text{S4.1})$$

This value is consistent with the results depicted in Fig.1(b) and Fig.2(b)]. By substituting this value, we derive the equation for the phase boundary,

$$J_c/E_c = \frac{\Delta^{-1}}{8d\gamma} e^{1 + \frac{\gamma}{4\Delta^{-1}}} \quad (\text{S4.2})$$

This equation also matches with the plots shown in Fig.1(b) and Fig.2(b). To find the threshold point, we minimize  $J_c$ , leading to

$$\left(\frac{\gamma}{\Delta^{-1}}\right)_{th} = 4 \quad (\text{S4.3})$$

This condition is also satisfied in Fig.1(b) and Fig.2(b). Substituting this in Eq.(S4.2), we obtain the threshold value of coupling to be  $J_{th} = \frac{e^2}{32d}$ , which only depends on the dimension  $d$ . Thus, the threshold value gets lowered in higher dimensions.

##### 1. Comparison between dissipative JJA model and measurement JJA model

We now contrast the monitored JJA with the Ohmic JJA. By comparing Eq.(S2.21) and Eq.(S3.6), it is evident that a zero effective temperature is not achievable in the monitored model, unlike in Ohmic JJA model. In the zero-temperature limit of the Ohmic model, the integrand of Eq.(S3.6) will depend linearly on  $\omega$ . However, the measurement model has quadratic dependence without any linear term in  $\omega$ . Additionally, the limit  $\Delta^{-1} \rightarrow 0$  while keeping  $\gamma^2/\Delta^{-1}$  a constant value in the monitored model has no analogous limiting case possible for the Ohmic JJA. The integrand in Eq.(S2.21) for the monitored model, only contains the term of the order  $\omega^2$ , which is unattainable by an expansion of  $\omega \coth(\omega/2T)$  (see Eq.(S3.6)) at any limit of  $\omega$  or  $T$  in the dissipative model. However, in that limit, the phase fluctuation of the measurement model in Eq.S2.21 diverges, always resulting in an insulating state.

We now investigate some more interesting similarities and differences between the two models. The high-temperature Ohmic model and the monitored model, at high effective temperature  $T_{eff}$ , exhibit similar behavior, as discussed in main text. In Figs.(1)(d,e), we compare the phase diagram of dissipative model in  $T - J$  plane with the phase diagram of the monitored model in  $T_{eff} - J$  plane. We observe that the phase diagram of the Ohmic model at higher temperatures closely resembles the monitored model at the same effective temperature. However, at lower temperatures, their behavior differs significantly. One can observe that the critical value of the coupling strength increases with the equilibrium temperature in the Ohmic JJA. However, in the monitored JJA, we see the re-entrant phase transition while varying the effective temperature. Beyond a certain threshold value of  $J/E_c$  we get an insulator-superconductor-insulator re-entrant phase transitions. At lower values of  $T_{eff}$ , we observe no global phase coherence. However, as the effective temperature rises above a critical value, it suppresses the phase fluctuations and restores superconductivity. Although at much higher effective temperatures, the model again fails to sustain the global phase coherence beyond a certain  $T_{eff}$ .

## S5: Limiting cases of monitored JJA model

In this section, we discuss the various limiting cases of monitored JJA model to confirm the qualitative aspects of the SCHA phase diagrams discussed in the main text.

### 1. Semi-classical limit of monitored JJA

We take the semi-classical limit of our model following procedure similar to that in Ref.51 for monitored oscillator chains. In the action of Eq.(1) (main text), we define  $\bar{\xi}_{ij} = \xi_{ij} - \Delta\theta_{ij,c}$  and scale  $\theta_{iq}$  and  $\bar{\xi}_{ij}$  as  $(\theta_{iq}/\hbar, \bar{\xi}_{ij}/\hbar) \rightarrow (\theta_{iq}, \bar{\xi}_{ij})$ . Subsequently, we expand the action  $S[\theta, \xi]$  in powers of  $\theta_{iq}$ , which is equivalent to expansion in powers of  $\hbar$ . To approach a non-trivial semiclassical limit with  $\hbar \rightarrow 0$ , we consider  $\Delta/\hbar^2$ ,  $E_c/\hbar^2$  to be finite in the limit  $\hbar \rightarrow 0$ , i.e.,  $\Delta$ ,  $E_c \sim \hbar^2$ ,  $\gamma \sim \mathcal{O}(\hbar^0)$  so that  $\theta_{ic}, \theta_{iq}, \bar{\xi}_{ij} \sim \mathcal{O}(1)$ . This ensures that both  $\bar{\xi}_{ij}$  and  $\Delta\theta_{ij,q}$  are Gaussian distributed with a width of  $\mathcal{O}(1)$  in the semi-classical limit. This also implies that  $\xi_{ij}(t) = \Delta\theta_{ij,c}(t) + \hbar\mathcal{O}(1)$ . Thus, the measurement outcomes  $\{\xi_{ij}(t)\}$  get pinned to  $\{\Delta\theta_{ij,c}(t)\}$  in the classical limit  $\hbar \rightarrow 0$  and only a single quantum trajectory contributes to time evolution of the system. Keeping the leading terms of  $\mathcal{O}(1)$ , we get,

$$\frac{S}{\hbar} = \int dt \left\{ \sum_i \left[ -2\frac{\hbar^2}{E_c} \ddot{\theta}_{ic} \theta_{iq} - 2\frac{\hbar^2\gamma}{E_c} \sum_{i \in \text{nni}} \theta_{iq} \Delta\dot{\theta}_{ij,c} - \sum_{j \in \text{nni}} 2\Delta\theta_{ij,q} \frac{\partial V}{\partial \Delta\theta_{ij,c}} \right] + \frac{i\hbar^2}{\Delta} \sum_{\langle ij \rangle} [\bar{\xi}_{ij}^2 + (\Delta\theta_{ij,q})^2] \right\} \quad (\text{S5.1})$$

where,  $V(\theta_{is} - \theta_{js}) = J(1 - \cos(\theta_{is} - \theta_{js}))$ . In the above, we have used integration by parts while performing the integration  $\int dt 2(\hbar^2/E_c) \dot{\theta}_{ic} \dot{\theta}_{iq}$  which becomes  $-\int dt 2(\hbar^2/E_c) \ddot{\theta}_{ic} \theta_{iq}$ , ignoring the boundary term. Similar integration is performed for  $\int dt \theta_{ic} \dot{\theta}_{iq}$  which becomes  $-\int dt \theta_{iq} \dot{\theta}_{ic}$ . Additionally, we have utilized  $\sum_i \dot{\theta}_{iq} \sum_{j \in \text{nni}} \xi_{ij} = \sum_{\langle ij \rangle} \Delta\dot{\theta}_{ij}^q \xi_{ij}$ . Using the Hubbard-Stratonovich identity we get

$$Z[\xi] \propto \int \mathcal{D}\eta \mathcal{D}\xi e^{-\frac{\hbar^2}{\Delta} \int dt \sum_{\langle ij \rangle} \bar{\xi}_{ij}^2} e^{-\frac{\Delta}{\hbar^2} \int dt \sum_{\langle ij \rangle} \eta_{ij}^2} \int \mathcal{D}\theta_c \prod_{it} \delta \left( \frac{\hbar^2}{E_c} \ddot{\theta}_{ic} + \sum_{j \in \text{nni}} \left( \frac{\hbar^2\gamma}{E_c} \Delta\dot{\theta}_{ij}^c + \frac{\partial V}{\partial \Delta\theta_{ij}^c} - \eta_{ij} \right) \right) \quad (\text{S5.2})$$

This leads to the classical stochastic Langevin equation for the classical component,  $\theta_c(t) \equiv \theta_{ic}(t)$

$$\frac{\hbar^2}{E_c} \frac{d^2\theta_i}{dt^2} = \sum_{j \in \text{nni}} \left[ -\frac{\hbar^2\gamma}{E_c} (\dot{\theta}_i - \dot{\theta}_j) - J \sin(\theta_i - \theta_j) + \eta_{ij} \right] \quad (\text{S5.3})$$

with a noise  $\eta_{ij}$ , which originates from quantum fluctuations  $\theta_{iq}$ . The noise has a Gaussian distribution controlled by the measurement strength  $\hbar^2/2\Delta$ , such that for  $\langle ij \rangle$ ,

$$\langle \eta_{ij}(t) \eta_{kl}(t') \rangle = \frac{\hbar^2}{2\Delta} \delta_{ik} \delta_{jl} \delta(t - t') \quad (\text{S5.4})$$

Here, we get  $T_{eff} = (\Delta^{-1}/4\gamma)E_c \sim \mathcal{O}(\hbar^0)$ . In the semiclassical limit, from Eq.(S2.21), we obtain  $\overline{\langle \Delta\theta_{ij,s}^2 \rangle}_v \simeq T_{eff}/dD + \mathcal{O}(\hbar^2)$ . As a result, from Eq.(2)(main text), we get

$$D \simeq J e^{-\frac{T_{eff}}{dD}} \quad (\text{S5.5})$$

Now we compare the classical limit of measurement model with the dissipative JJA model. In the high-temperature limit of the dissipative JJA model, we consider the expression of the phase fluctuation neglecting  $\mathcal{O}(1/T)$  terms and beyond in Eq.(S3.6). We obtain the phase fluctuations to be  $\langle \Delta\theta_{ij}^2 \rangle_{\text{var}} \simeq 2T/dD$ . Thus, the self-consistent equation becomes,  $D \simeq J \exp[-(T/dD)]$ . This expression is the same as Eq.(S5.5) for the monitored model in the semi-classical limit at effective temperature  $T_{eff}$ . Hence in the classical limit, both the monitored and dissipation cases exhibit the same behavior.

### 2. Strong feedback and measurement limit of the monitored JJA

As discussed earlier, the feedback  $\gamma$  acts like a dissipation in the monitored JJA. Thus, in the large feedback limit, we expect the system to behave classically, with weak time dependence of the phases to avoid large action [Eq.(1)]



(main text)] due to the damping term in the effective action, e.g., as in the SCHA effective action of Eq.(S2.15). In this limit, we decompose the phases into slow and fast modes,

$$\begin{aligned} \text{Fast modes:} \quad \theta_{i\alpha}^>(t) &= \int_{\omega_c \leq |\omega| \leq \omega_m} \frac{d\omega}{2\pi} e^{-i\omega t} \theta_{i\alpha}(\omega) \\ \text{Slow modes:} \quad \theta_{i\alpha}^<(t) &= \int_{0 \leq |\omega| \leq \omega_c} \frac{d\omega}{2\pi} e^{-i\omega t} \theta_{i\alpha}(\omega) \end{aligned} \quad (\text{S5.6})$$

where  $\alpha = c, q$  and the lower cutoff  $\omega_c = JE_c/\hbar^2\gamma$  is obtained by comparing the JJ term with the effective damping term, i.e.,  $J \sim (\hbar^2\gamma/E_c)\omega_c$ . We set the upper cutoff,  $\omega_m = \gamma$ , by the feedback term, but it can also be set to  $\Delta^{-1}$ , leading to qualitatively same results. We also make the same division into fast and slow variables for the measurement fields  $\{\xi_{ij}(t)\}$ . The next step is to express the action in terms of fast and slow components of the classical and quantum fields  $(\theta_{ic}, \theta_{iq})$ . It is sufficient to expand the JJ term in the action up to first order in the quantum component and second order in the classical component. Every other term in the action, being quadratic, split into terms involving only slow and fast components. Hence, the action can be approximated as,

$$S[\theta, \xi] \approx S_0^<[\theta^<, \xi^<] + S_0^>[\theta^>, \xi^>] + \frac{1}{2} \left[ \frac{\partial^2 V}{\partial \Delta \theta_{ij}^2} \right]_{<} (\Delta \theta_{ij,c}^> \Delta \theta_{ij,q}^> + \Delta \theta_{ij,q}^> \Delta \theta_{ij,c}^>) + \frac{1}{6} \left[ \frac{\partial^3 V}{\partial \Delta \theta_{ij}^3} \right]_{<} (6(\Delta \theta_{ij,c}^>)^2 \Delta \theta_{ij,q}^>) \quad (\text{S5.7})$$

where  $S_0$  is the quadratic part of the action in Eq.(1) (main text). In Eq.(S5.7), we can treat the second and higher-order terms perturbatively. Now, we integrate out the fast degree of freedom and get a trajectory-averaged generating function in terms of only slow degrees of freedom,

$$\mathcal{Z} \sim \int \mathcal{D}\theta^< \mathcal{D}\xi^< e^{\frac{i}{\hbar} S^<} \left\langle \exp \left( -\frac{i}{\hbar} \int dt \left[ \frac{1}{2} \left[ \frac{\partial^2 V}{\partial \Delta \theta_{ij}^2} \right]_{<} (\Delta \theta_{ij,c}^> \Delta \theta_{ij,q}^> + \Delta \theta_{ij,q}^> \Delta \theta_{ij,c}^>) + \left[ \frac{\partial^3 V}{\partial \Delta \theta_{ij}^3} \right]_{<} (\Delta \theta_{ij,c}^> \Delta \theta_{ij,q}^>) \right] \right) \right\rangle_{>} \quad (\text{S5.8})$$

$$\approx \int \mathcal{D}\theta^< \mathcal{D}\xi^< e^{\frac{i}{\hbar} S^<[\theta^<, \xi^<]} \exp \left( -\frac{i}{\hbar} \int dt \left[ \frac{\partial^3 V}{\partial \Delta \theta_{ij}^3} \right]_{<} \langle (\Delta \theta_{ij,c}^>)^2 \rangle_{>} \Delta \theta_{ij}^< \right) \quad (\text{S5.9})$$

In the above, we have used a cumulant expansion, keeping the lowest-order term, and used  $\langle \Delta \theta_{ij,c}^>(t) \Delta \theta_{ij,q}^>(t) + \Delta \theta_{ij,q}^>(t) \Delta \theta_{ij,c}^>(t) \rangle_{>} \sim G^{R,>}(t, t) + G^{A,>}(t, t) = 0$  and  $\langle \Delta \theta_{ij,c}^>(t) \rangle_{>} = 0$ . Here

$$\begin{aligned} \langle (\Delta \theta_{ij,c}^>)^2 \rangle_{>} &= \frac{2\hbar}{Nd} \sum_{\mathbf{q}} \int_{E_c J/\hbar^2\gamma}^{\gamma} \frac{d\omega}{2\pi} \left( \frac{\hbar\Delta^{-1} + \frac{\hbar^3\gamma^2\omega^2}{E_c^2\Delta^{-1}}}{2(\hbar^4\omega^4/E_c^2 + \hbar^4\gamma^2\omega^2 K^2(\mathbf{q})/E_c^2)} \right) K^2(\mathbf{q}) \\ &\approx \frac{2}{Nd} \sum_{\mathbf{q}} \left( \frac{K(\mathbf{q})\gamma}{8\Delta^{-1}} + \left( \frac{E_c\Delta^{-1}}{\hbar^2} \right) \frac{2K(\mathbf{q})\hbar^2\gamma^2 - \pi J E_c}{8\pi K(\mathbf{q})J\gamma^3} \right) \end{aligned} \quad (\text{S5.10})$$

In this procedure, we get the action that looks the same as the original action of Eq.(1)(main text) with an additional term  $-\frac{i}{\hbar} \int dt \left[ \frac{\partial^3 V}{\partial \Delta \theta_{ij}^3} \right]_{<} \langle (\Delta \theta_{ij,c}^>)^2 \rangle_{>} \Delta \theta_{ij}^<$ . As in the semiclassical limit of Sec.S5.1, we again define  $\bar{\xi}_{ij}^< = \xi_{ij}^< - \Delta \theta_{ij,c}^<$ . However, in this case, we scale  $\bar{\xi}_{ij}^<$  as  $\sqrt{\hbar\Delta^{-1}} \bar{\xi}_{ij}^< \rightarrow \bar{\xi}_{ij}^<$ . As a result, in the limit of large measurement strength  $\hbar\Delta^{-1} \gg J, E_c$ , keeping the leading order term in  $\hbar\Delta^{-1}$  and following the similar Hubbard-Stratonovich decoupling procedure as in Sec.S5.1, we get a Langevin equation for the slow modes,  $\theta_{ic}^< \equiv \theta_i^<$ ,

$$\frac{\hbar^2}{E_c} \ddot{\theta}_i^< = \sum_{j \in \text{nni}} \left[ -\frac{\hbar^2}{E_c} \gamma (\dot{\theta}_i^< - \dot{\theta}_j^<) - J_{eff} \sin(\theta_i^< - \theta_j^<) + \eta_{ij} \right] \quad (\text{S5.11})$$

where the effective JJ coupling is given by

$$J_{eff} = J \left( 1 - \frac{\langle (\Delta \theta_{ij,c}^>)^2 \rangle_{>}}{2} \right) \quad (\text{S5.12a})$$

$$\approx J \left( 1 - \frac{\gamma}{4\Delta^{-1}} \right) \quad \gamma \gg \Delta^{-1} \quad (\text{S5.12b})$$

$$\approx \left( 1 - \frac{\Delta^{-1} E_c}{4\pi d \gamma J} \right) \quad \Delta^{-1} \gg \gamma \quad (\text{S5.12c})$$

### 3. Weak-JJ-coupling limit of the monitored JJA

In this limit, we treat the JJ term in the action of Eq.(1) (main text) perturbatively and employ the weak-coupling renormalization-group (RG) scheme to obtain the RG flow equation for JJ coupling. To this end, we define the slow and fast modes of the fluctuating phase  $\theta_{i\alpha}(t)$  ( $\alpha = c, q$ ) as,

$$\text{Fast modes:} \quad \theta_{i\alpha}^>(t) = \int_{\omega_c/b < |\omega| < \omega_c} \frac{d\omega}{2\pi} e^{-i\omega t} \theta_{i\alpha}(\omega) \quad (\text{S5.13a})$$

$$\text{Slow modes:} \quad \theta_{i\alpha}^<(t) = \int_{-\omega_c/b}^{\omega_c/b} \frac{d\omega}{2\pi} e^{-i\omega t} \theta_{i\alpha}(\omega), \quad (\text{S5.13b})$$

and similarly for the measurement fields  $\{\xi_{ij}(t)\}$ . Here  $\omega_c$  is the cutoff frequency depending on the largest energy scale between  $E_c$ ,  $\hbar\gamma$  and  $\hbar\Delta^{-1}$ , and  $b = e^{\delta l} > 1$ . In the perturbative RG scheme, we consider the expansion involving  $J/E_c$  up to first order. After integrating out the fast variables, the generating function can be expressed as,

$$\mathcal{Z} \sim \int \mathcal{D}\xi^< \mathcal{D}\theta^< e^{\frac{i}{\hbar} S_0^<[\theta^<, \xi^<]} \left\langle e^{\frac{i}{\hbar} \sum_s s \int_{-\infty}^{\infty} dt \sum_{<ij>} J \cos(\theta_{is} - \theta_{js})} \right\rangle_{>} \quad (\text{S5.14})$$

$$\approx \int \mathcal{D}\xi^< \mathcal{D}\theta^< e^{\frac{i}{\hbar} S_0^<[\theta^<, \xi^<]} e^{\frac{i}{\hbar} \sum_s s \int_{-\infty}^{\infty} dt \sum_{<ij>} J \cos(\Delta\theta_{ij,s}^<) e^{-\frac{1}{2} \langle (\Delta\theta_{ij,s}^>)^2 \rangle_{>}} \quad (\text{S5.15})$$

Here,  $S_0^<[\theta^<, \xi^<]$  is the action incorporating only the slow variables, setting the coupling to be 0. Next, we rescale  $(\theta_{is}(\omega), \omega, t, E_c) \rightarrow (\theta_{is}(\omega)/b, \omega b, t/b, E_c b)$ . This results in a similar expression for action with a rescaled JJ coupling by  $J' = J b e^{-\frac{1}{2} \langle (\Delta\theta_{ij,s}^>)^2 \rangle_{>}}$ , where

$$\langle (\Delta\theta_{ij,s}^>)^2 \rangle_{>} = \frac{\hbar}{Nd} \sum_{\mathbf{q}} \int_{\omega_c/b \leq |\omega| \leq \omega_c} \frac{d\omega}{2\pi} \frac{K^2(\mathbf{q})(\hbar\Delta^{-1} + \frac{\hbar^3\gamma^2\omega^2}{E_c\Delta^{-1}})}{\hbar^4\omega^4/E_c^2 + \hbar^4\gamma^2\omega^2 K^2(\mathbf{q})/E_c} \quad (\text{S5.16})$$

Performing infinitesimal RG transformation  $b = e^{\delta l} \approx 1 + \delta l$ , we obtain the differential RG flow equation for  $J$ . For notational convenience, we define dimensionless quantities  $\tilde{\gamma} = \hbar\gamma/E_c$  and  $\tilde{\Delta}^{-1} = \hbar\Delta^{-1}/E_c$  below.

For  $\hbar\gamma$  the largest energy scale, we take  $\omega_c = \gamma$ . Taking  $\hbar\gamma$  much larger than other energy scales, we simplify the evaluation of  $\langle (\Delta\theta_{ij,s}^>)^2 \rangle_{>}$  by ignoring the  $\omega^4$  term in the denominator of Eq.(S5.16) to get  $\langle (\Delta\theta_{ij,s}^>)^2 \rangle_{>} = \frac{1}{2\pi\tilde{\gamma}d} \left( \frac{\tilde{\Delta}^{-1}}{\tilde{\gamma}^2} + \frac{\tilde{\gamma}^2}{\tilde{\Delta}^{-1}} \right) \left( 1 - \frac{1}{b} \right)$ . This gives the RG flow equation,

$$\frac{dJ}{dl} = J \left( 1 - \frac{1}{4\pi\tilde{\gamma}d} \left( \frac{\tilde{\Delta}^{-1}}{\tilde{\gamma}^2} + \frac{\tilde{\gamma}^2}{\tilde{\Delta}^{-1}} \right) \right), \quad (\text{S5.17})$$

leading to the  $\beta$  function mentioned in the main text. In the case, where  $E_c$  is the dominant energy scale, we cannot simply neglect the  $\omega^4$  term in the denominator of the integrand in Eq.(S5.16). However, we can still integrate out the modes between  $\hbar\gamma < |\omega| < E_c$  to get an effective action whose upper frequency cutoff is determined by  $\gamma$ . This procedure merely multiplies a prefactor to the JJ term, keeping the same flow equation as above with an effective  $J$ . Hence we get the same RG flow equation Eq.(S5.17) also in this limit.